UNIVERSITY OF CALIFORNIA

Los Angeles

Interaction-Powered Internet of Things

A thesis submitted in partial satisfaction

of the requirements for the degree

Master of Science in Electrical and Computer Engineering

by

Xiaoying Yang

2023

ABSTRACT OF THE THESIS

Interaction-Powered Internet of Things

by

Xiaoying Yang
Master of Science in Electrical and Computer Engineering
University of California, Los Angeles, 2023
Professor Yang Zhang, Chair

As we are quickly heading towards a trillion device Internet-of-Thing (IoT), it becomes crucial to develop zero-maintenance and long-life ubiquitous IoT systems, eliminating the need for batteries and maintenance. To address this issue, researchers have been investigating harvesting energy from various ambient energy sources, such as sunlight, thermal gradients, and RF sources, to power IoT devices and enable self-sustainability. In this thesis, we explored generating power from a unique energy source – user interactions, and utilized the power to enhance the actuation and sensing capabilities of IoT devices. We investigated the characteristics of interaction energy from everyday objects and the factors that affect them. We designed a wide variety of mechanical mechanisms that are retrofittable to everyday objects to harvest kinematic energy from user interactions. To perform IoT sensing and actuation, we equipped them with motors capable of alternating between harvester and actuator for motorization, and computationally designed retro-reflectors for wireless backscatter. We evaluated both systems with deployment studies, which proved the efficacy of our systems as well as shedding light into this interaction-powered approach as a feasible solution to address energy needed for IoT applications.

The thesis of Xiaoying Yang is approved.

Mani B. Srivastava

Xiang Chen

Yang Zhang, Committee Chair

University of California, Los Angeles

2023

TABLE OF CONTENTS

LIST OF FIGURES

LIST OF TABLES

ACKNOWLEDGMENTS

I would like to express my sincerest gratitude to my advisor, Yang Zhang, for his invaluable guidance and immense support throughout my research journey. His expertise, insights and encouragement have been essential in shaping me into not just a researcher but also a better person. I am also grateful to Josiah Hester for his generous support and constructive feedback during the completion this thesis. I would also like to thank my thesis committee members, Mani Srivastava and Xiang Chen, for their valuable feedback and insights.

I am grateful to my collaborator, Jacob Sayono, whose enthusiasm and creativity have continually inspired me, turning the research process into an adventure filled with surprises and discoveries. I would like to thank my colleagues, Siyou Pei and Xue Wang, for the friendship and kindness they offered, and for being attentive and supportive listeners through both the ups and downs of my life.

I would like to thank my furry friend Boba for his unconditional trust and love. His comforting meows and purrs have been a constant source of healing and joy during the challenging period of my studies. I am thankful to my partner, whose companionship, understanding and love have provided immeasurable comfort and gain me emotional stability during these years, inspiring me to embrace the brighter sides of life and leave the darker moments behind.

Finally, I would like to express my deepest and most profound gratitude to my parents, particularly my mother. Her dedication to our family and the responsibilities she has shouldered day after day have been a source of strength for me; without her support completing this degree would have been an impossible task.

I feel immensely fortunate for the support I have received throughout my life of over twenty years from family, mentors, friends, and sometimes even strangers. I am deeply thankful for everything and everyone who has been a part of this journey, and I eagerly look forward to the next phase of my academic journey.

CHAPTER 1

Introduction

1.1 Background

In recent decades, we have been quickly heading towards a Internet-of-Things (IoT) era, where a trillions of smart devices are expected to deploy in future environments communicating with each other to form an intelligent IoT network. Sensing serves as the input for the IoT network, gathering personal and environmental data such as human activities, noise levels and air quality, to comprehend the surrounding context. Actuation, on the other hand, acts as the output, carrying out physical actions in response. For example, smart doors, smart curtains and smart coffee machine automate various processes, minimizing the effort required to operate these household appliances.

The explosion of these computing devices has prompted the reevaluation of the reliance on batteries as power sources, which currently serve as the primary energy solution for existing IoT devices. The need for periodic maintenance of batteries in these trillion-level, diverse devices results in extremely high labor costs, which presents a major challenge in the large-scale deployment of IoT devices. In light of this, considerable research has been conducted on replacing batteries with energy harvesters that can continuously gather energy from the environment such as sunlight, thermal gradients and RF sources. These efforts contribute to extending the lifespan of IoT devices and have demonstrated effectiveness.

In contrast, this thesis explores sourcing power from people, specifically harnessing kinetic energy generated during people interactions with everyday objects. This kinetic energy

will undoubtedly be present wherever there are user interactions with objects, such as opening/closing the doors and rotating the tilt wand of window blinds, which can accumulate to a substantial amount of power. Unlike kinetic harvesters that necessitate deliberate user actions to generate power for subsequent tasks, interaction power harvesters operates without altering the original tasks users performs, picking up the energy that otherwise dissipates while minimizing the interaction overhead.

The core of kinetic energy harvesting lies in the electromagnetic induction effect, converting motions into electricity. Actuation operates oppositely, using electricity to create motion. This offers unique benefits for using interaction power for IoT actuation - an interaction power harvester can be repurposed as an actuator to perform actuation tasks. This thesis leveraged interaction power for actuation by enabling motors to work as both harvesters and actuators seamlessly in a smart environment, allowing self-sustainable robotic IoT devices (Chapter 3).

The utility of interaction power can be further enhanced by the fact that it inherently contains substantial information about user activities such as state, direction, rate and count. This thesis leveraged interaction power as sensory feeds through both explicit and implicit methods. Information about user activities can be extracted from the interaction power pattern such as direction and magnitude (Chapter 3). Furthermore, in light to the growing significance of wireless sensing in IoT, we proposed transforming interaction power into structured responses to millimeter wave radar using corner reflector mechanisms, facilitating the implicit utilization of interaction power for user activity detection (Chapter 4).

Overall, the goal of this thesis is to **harness interaction power for self-sustainable IoT sensing and actuation**. This thesis designed, developed and evaluated systems for real-world applications and demonstrated the feasibility of the proposed approach.

1.2 Thesis Outline

This thesis is organized as follows.

In **Chapter 2**, we conducted benchmark tests to examine the characteristics of interaction power. We investigated the amounts of energy that could be harvested from everyday objects and the factors that affect them, including configurations of harvesters and characteristics of user motions. We also measured the energy consumption in automatic operations of smart home devices. The findings from these tests provide valuable insights into implementations of smart actuation and sensing systems for IoT applications using interaction power.

In **Chapter 3**, we presented the utilization of interaction power as a source of energy for a fleet of environmental automation devices, achieving self-sustaining automatic operations. We developed a custom circuit that features power management, programmable motor powerline resistance, PWM motor drive, event-triggered sensing and computation, nonvolatile memory, and BLE communication. We also developed two phone apps, one for interactive control and the other for data management. A series of technical validations and a 48-hour deployment study were conducted to prove the efficacy of our system.

In **Chapter 4**, we introduced the use of interaction power to facilitate wireless sensing of human activities in IoT. We demonstrated a computational approach to design passive reflector mechanisms that can encode activities into characteristic mmWave reflections. We conducted a study at three different locations, which demonstrated the robustness of our approach with extremely low false positive rates across distances and angles.

Chapter 5 concludes this thesis by reflecting on our exploration on interaction power for IoT applications. We also presented our vision for the practical implementation of our systems and discussed potential avenues for future research on this topic.

CHAPTER 2

Energy Investigation

2.1 Overview

This chapter aims to investigate the characteristics of interaction power, the factors that affect energy harvesting, and the power consumption for common IoT actuation tasks. We conducted benchmark tests to answer: how does the amount of energy harvested from manual operations compare to that of the energy consumed in automatic operations? These tests are essential for comprehending interaction power, playing a significant role in guiding the development of IoT actuation and sensing systems throughout this thesis.

2.2 Apparatus

We conducted benchmark tests to investigate amounts of energy that could be harvested from everyday objects as well as the factors that affect them. To conduct these tests with sufficient versatility without losing generalizability, we decided to use a 3D printed device (Figure 2.1 right). This 3D printed device allowed us to correlate harvested energy with force (in translational motions) and torque (in rotational motions), in forms that are common to find in everyday settings (Figure 2.1 left). The device can be put into two configurations. The first configuration features a handle that moves in a translational manner while the second configuration features a handle that moves in a rotational manner, both in relation to the device body. The force and torque needed to actuate the device are set by the embedded motors, for which we selected the GA12-N20 DC motor with an additional gearbox

attachment. This type of motor is low-cost and easy to source, because of which they are common to find in maker projects and commercial products.

Figure 2.1: Translational and rotational motions are the two common types of motion on everyday objects (left). The device designed to simulate these motions on everyday objects and used in the energy investigation tests (right).

2.3 Factors

2.3.1 Motor Gear Ratio

One immediate factor that affects energy harvesting is the gear ratio of the gearbox, which is the ratio between the angular speeds of the driver (input) gear to the driven (output) gear. Of note that when motors are used as generators, the driven gear is the one that is actuated by user interactions, and therefore the gear ratio becomes the reciprocal of that of motors as actuators. Intuitively, larger gear ratios require a larger force to actuate but can induce a higher amount of energy. We conducted tests to quantify this effect in the context of user-powered mechanisms. In this test, we used motors with gearboxes of different gear ratios (500:1, 250:1, 150:1, 100:1, 75:1) and measured their output currents when these motors were connected in series with a 100 Ohm resistor. These motors were instrumented onto the test

device, which was affixed to a lab table with the configuration that supports translational motions. An experimenter actuated the device from one end to the other and returned to the original position (i.e., one trial) three times at normal speeds (similar to ones in actuating everyday objects) during which a force gauge was used to measure force and torque. Figure 2.2 left shows the results, which verified our expectation that the force required and energy generated are proportional to the gear ratio – motors with larger gear ratios are in general harder to actuate, but can generate more energy which is roughly linearly proportional to the gear ratio.

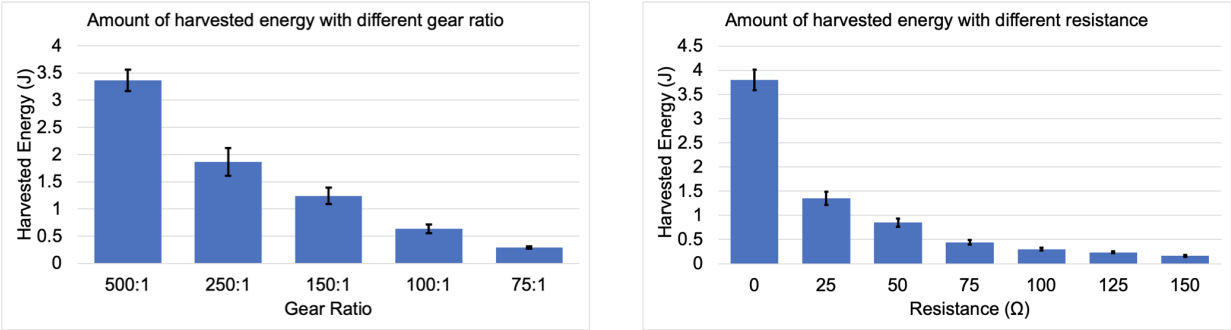

Figure 2.2: Investigation of gear ratio's effect on harvested energy (left). Investigation of the effect on harvested energy from the resistance in the motor powerline (right).

2.3.2 User Motion Characteristics

An important factor that affects energy harvesting is the varying user interactions due to the fact that different users often have different motor capabilities, resulting in different speeds, acceleration and deceleration rates, etc. This variance could affect the amount of harvested energy. We conducted a user study (n=5), using the same device in the previous test. A motor with the gearbox of a 250:1 ratio was used. Its output was connected to a 100 Ohm resistor. Participants were asked to complete three trials actuating the device at normal speeds. The output voltage across the resistor was recorded and can be found in Figure 2.3. Interestingly, we measured a largely consistent amount of generated energy

despite that different users manipulated the device at different speeds. However, we found a large difference between the two motion types – translational motions generate more energy than rotational motions due to the difference in the number of revolutions by the motor over the courses of trials. This observation led to the design of having larger gear ratios for rotational motions than translational ones later in our system implementation.

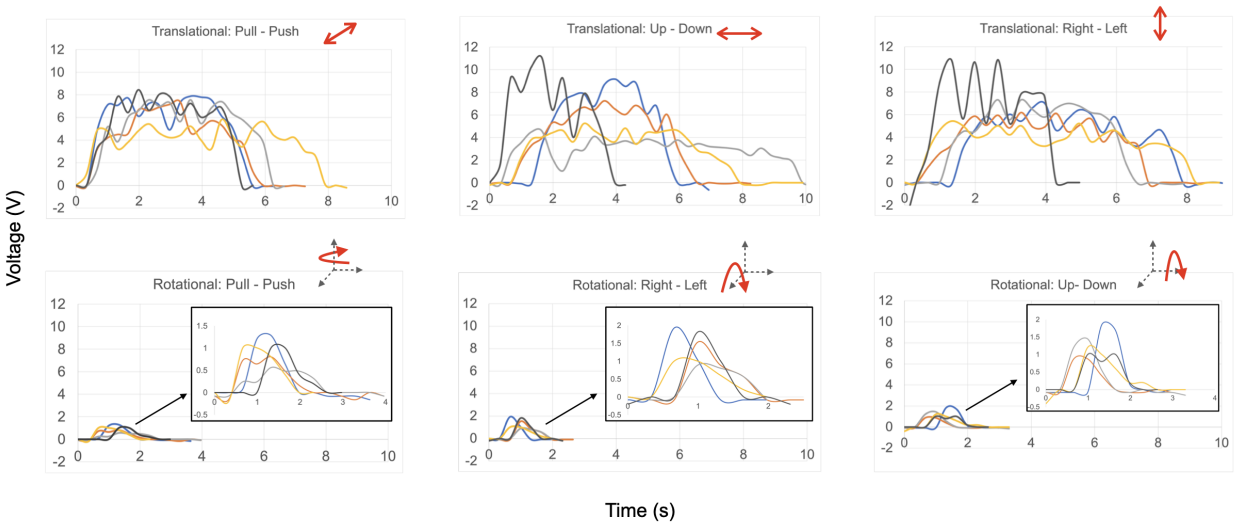

Figure 2.3: Signal characteristics of interaction-powered motor mechanisms with two motion types: translational and rotational. Each color denotes data from one participant.

2.3.3 Resistance in Motor Powerline

Resistance in the motor powerline affects the output currents and thus the harvested energy. In practice, we found that increasing this resistance limits the output currents by motors and reduces the force and torque to actuate the mechanisms. This correspondence gives us a way of setting motor force/torque in a finer-grained manner using programmable resistors than using gearboxes, because gearboxes often have discrete gear ratios and are impossible to change by software. In this test, we connected the motor in series with a resistor. The device was configured to support translational motions and we used a gearbox of a 250:1 ratio. A capacitor of 2.5 F was connected to the motor-resistor setup for storing the harvested

energy, which can be calculated by measuring the voltage increases using a multimeter. We gradually changed the amount of current generated by motors by changing the resistance (from 0 to 150 Ohm with a 25 Ohm interval). This change in induced current also changed forces needed to actuate the device, which we measured with the force gauge. Figure 2.2 right shows measurements of amounts of energy in response to the change of resistance. We found that the device was harder to actuate with a lower resistance value (in series) but can generate more energy. For example, a 100 Ohm resistor can reduce 54% of the total force required to move the device.

2.4 Energy Measurement

2.4.1 Harvest Energy from Real-World Objects

Previous tests outline the characteristics of interaction-powered harvested energy. To gauge more precisely how much energy can be harvested from users' interactions with everyday objects, we conducted tests on real everyday objects. We included 9 common objects, with 5 involving rotational motions (i.e., fridge door, CNC enclosure, window blinds, toilet lid, room door) and 4 involving translational motions (i.e., backdrop, drawer, trash can, dimmer switch). We designed 3D-printed gear mechanisms that turn both types of motions into motor revolutions (Figure 3.3). Details of these mechanisms will be discussed later in the paper (Section 3.4.3). We used the motor with a gear ratio of 250:1 in tandem with these mechanisms. An experimenter manually operated these objects and measured the harvested energy of each object in one trial. On average, each trial of manually operating these objects generated 0.56J (SD=0.32) energy. Figure 2.4 shows the voltage across a 100 Ohm resistor in series with the motors of these objects being manually operated in one direction. We omit the rest of the trial for them simply mirroring the signals shown around the 0V line. In general, these half trials took from around 1 to 14 seconds to complete. Objects with longer strokes (e.g., backdrop, window blinds) generated more power for inducing more revolutions

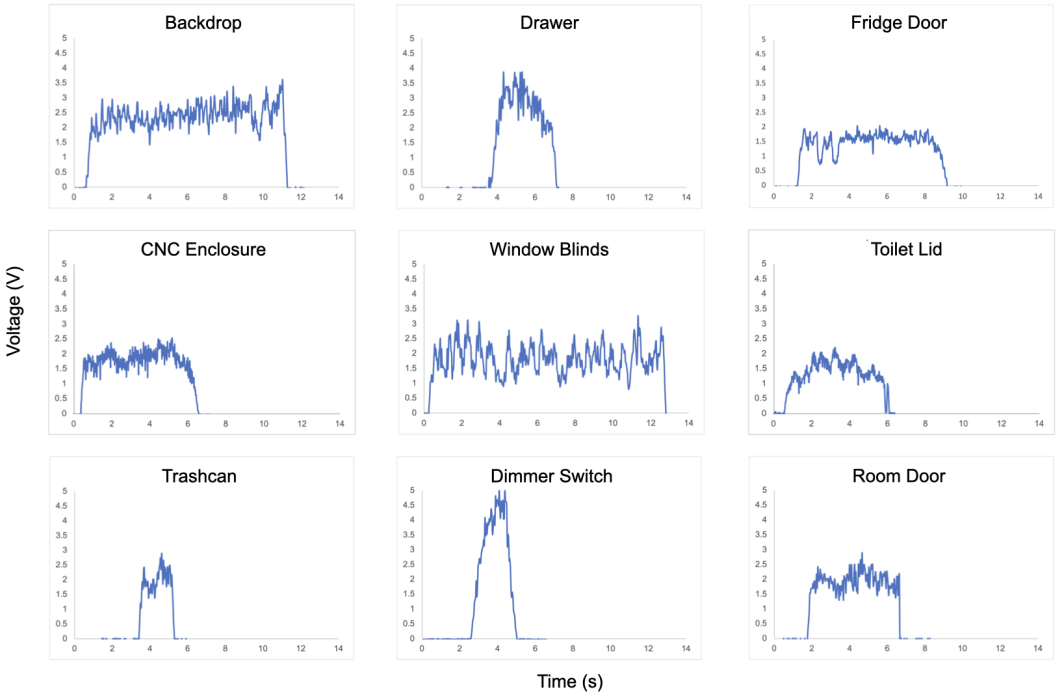

Figure 2.4: Voltage-time plot of the 9 objects with gear mechanisms and motors (gear ratio = 250:1) attached. These objects were manually operated from one extreme position to the other (i.e., half trials).

of motors, than those with shorter strokes (e.g., dimmer switch, trash can).

2.4.2 Energy Consumed for Actuating Real-World Objects

Previous tests help us understand how much energy can be harvested from user interactions. Here, we investigate energy consumption in automatic operations – how much energy we need to actuate objects. With the same set of objects in the previous test, we used a DC power supply (DCV=4V) to power the motors, which induced sufficient torque to actuate these objects at normal speeds. We measured the current during the courses of object actuation in three trials.

On average, these objects consumed 2.77 J (SD=2.03) energy in one trial of their actua-

tion (i.e., open and close). Similar to insights from the energy harvesting test, objects with longer strokes consumed more power for taking longer to complete the motion. Even on the same objects, actuation in different directions could consume different amounts of energy depending on if gravity contributes or resists the motion. For example, it takes 1.7 J on average to open a CNC enclosure door, while that number is 0.3 J for closing it. We also noticed that when the gear mechanisms were blocked by the objects from further movements at the completion of motion, motors were overloaded and drew a high current (i.e., stall current). This stall current measured approximately 120 mA with our motor, and consumed a lot of energy, for which we later designed our system so it can detect and cut off power timely to minimize energy wasted on unnecessary actuation.

CHAPTER 3

Interaction-Powered Mechanisms for Smart Environment Actuation

3.1 Introduction

Automating objects in physical spaces has long been practiced in ubiquitous computing and the Internet of Things. Automation not only boosts efficiency but also creates environments that can be equally accessible to all. These environments feature physical interfaces on the objects for manipulation or function (e.g., a handle or pedal for movement). Many everyday objects require users with enough dexterity, motor strength, and often the use of both hands to interact purposefully. These requirements can be challenging to someone who is not capable of such interaction due to a physical disability. Thus, automation can be a great benefit for users with motor impairments and even offer much utility to everyone else – for example, if someone has their hands occupied at the moment. Existing approaches (like sliding doors in a supermarket, automatic hand sanitizer dispensers in a building) rely either on tethered power, which limits the flexibility of deployment, or run on batteries demanding maintenance efforts. Both of these power solutions are difficult to scale – which we suspect to be one of the key reasons why we have only seen the success of automation on a few objects while the majority of everyday objects remain passive.

Prior research has tackled the energy challenges on the sensing front [CD14, CLC10, ZIJ19a, ZPZ20a] while little has been done on the actuating front – specifically in regards to actuating objects with intrinsic motion parameters (e.g., drawers with slides, doors with

hinges, etc.). This characteristic is a huge challenge as actuating applications require a large power consumption relative to sensing applications in many orders of magnitude. For instance, we found anecdotally that the amount of energy consumed to open a door once is equivalent to the amount of energy required to sense that event for nearly one whole year.

Fortunately, the remedy can be found in the problem. Electric motors consume energy when actuating objects; however, when used as generator, they are also ideal for harvesting energy from the current generated by the input actuation – the electromagnetic induction effect, which generates more than 93 % of all the electricity that powers the world [Dat22]. Our research uniquely leverages this advantage of motors by enabling them to work as both harvesters and actuators seamlessly in a smart environment. Our system intelligently switches between manual and automation modes depending on the user needs in the environment. One existing example of such design concept can be found on the commercially available door closers – energy stored in the spring when the door is being manually opened can later be used to automatically close it, preserving user time while improving environmental safety, achieved with a simple and passive device that can last for years [clo22]. Though door closers create force/torque overheads that might make it harder to use the door than without, the benefits overcome this potential undercut in usability. We were inspired by examples like this when we created our system, which generalize the design concept to a wide array of everyday objects.

This dual usage allows us to explore how we can utilize user interactions as a ubiquitous and reliable source of power. While prior work has demonstrated the efficacy of environment-centric harvesters (e.g., solar cells, wind turbines), we turned our focus to people – a rich source of kinetic energy – because there will undoubtedly be presence of users wherever there are interactive systems, and user interactions can be turned into power as several seminal works have demonstrated [ZIJ19a, VH10, DKH20, KPF13]. Unlike prior work which focused on interactive sensing, this thesis looks into a different and yet important task – actuation via enhancing objects that have intrinsic movements, with motors that can be repurposed

into energy harvesters.

We present MiniKers, a series of interaction-powered actuation devices for smart environment automation. MiniKers can retrofit to everyday objects with various mechanical mechanisms (see Figure 3.3 for examples) and feature a custom circuit board, energy-aware software, and a phone app. Taking the instrumented window blinds for example, MiniKers harvest energy from a synchronously spinning DC motor each time the tilt wand is turned manually. This energy is stored in a supercapacitor and then in a small Li-Po battery. This energy is later extracted from the battery to drive the same DC motor, providing the actuation force that turns the tilt wand and opens/closes the window blinds automatically. The energy harvesting, regulation, and management are controlled by the custom circuit board centered around low-power components including a BLE-enabled SoC (Nordic nRF52832). Simultaneously, our system hitchhikes the energy harvesting mechanism for sensing, turning the harvested energy into sensory feeds. Specifically, by monitoring the amount of harvested energy, MiniKers detect the state of objects as well as fine-grained information such as magnitude, speed, and frequency.

Overall, the contributions of this chapter include:

- Generalization of the design concept which uses people as power for interactive systems by harvesting energy from user interactions (i.e., manual operations) to power automatic operations of everyday objects.
- A custom circuit that uniquely combines sensing, energy harvesting, regulation, management, and energy-aware actuation for an optimal energy efficiency.
- A system that utilizes this custom circuit with various mechanical mechanisms that can cheaply retrofit onto everyday objects.
- A technical validation and a deployment study that assess the feasibility of interaction-powered automation, creating footholds for future work.

3.2 Related Work

3.2.1 Motorized Smart Environments

MiniKers are related to systems that actuate users' environments on their behalf, motorizing objects for remote controls or assisted uses. These systems intersect with research and commercial efforts in smart homes, automation, remote control, and personal robots. In the product domain, Clicbot [Key22], Smartians [Stu22], and Microbot-push [Mic22] use gear mechanisms powered by DC motors to enable remote actuation of everyday objects, mostly small ones like switches. There have also been automatic door closers [clo22] and greenhouse auto vent openers [See22] that actuate objects with only passive mechanisms (i.e., no electronic components). The aforementioned retrofitting devices could result in additional installation labor which can make built-in control mechanisms preferable if the "smarts" could be built from scratch (e.g., smart switch [Kas22] or smart lock [Q22]).

In the research domain, there have been two common modalities to achieve environment automation. People can either have general-purpose robots which can move around the space for a variety of tasks [KYT19, FEP16, KGP18, BOC18, ERZ01, BCD08, WLC18], or robotic mechanisms which can be instrumented onto objects for software-controlled actuation [LKC19, LCK20, LSK22, ALC22, HJ14, RAG16, CKL21]. The latter is more closely related to this work. In this realm of innovations, IoTIZER [CKL21] instruments light and aesthetically appealing mechanisms onto objects with a toolkit. Robiot [LKC19] motorizes everyday objects by retrofitting 3D-printed motor mechanisms. Mobiot [ALC22] further mobilizes the objects with 3D-printable structures. In this line of work, Roman [LSK22] enables handheld objects to be manipulable by robotic arms with 3D-printable add-on mechanisms. It is possible to structurally modify everyday objects to augment their default functionalities [LCK20, HJ14]. Finally, RetroFab [RAG16] offers an authoring tool to scan an existing physical interface and automate its controls by adding external mechanical and electronic components.

3.2.2 Power from Environments

Energy harvesting has long been exploited by interactive systems and environments in which these systems reside have many types of energy to leverage. One of the most common energy sources is light, harvested by photovoltaic panels. On commercial products, light energy harvesting is often used to extend battery lifetime. These products range from keyboards [Log21], smart curtains [Swi22] and cleaning robots [JGe17] to trash cans [lab22], street lights [Int22] and vehicles [Tes22].

In the research domain, a variety of energy sources have been utilized. Light continues its popularity as a major energy source in ubiquitous computing and IoT, powering systems for ambient displays [GHC16], hand posture reconstruction [LLP18], and touch sensing [WXZ20]. It is possible to harvest energy using piezoelectric materials from mechanical oscillations such as vibrations resulting from running motors [ZIJ19a], traffic on road and bridges [PS13, WJC18], fluctuations of pressure inside water pipes [CLC10], and even temporal ambient temperature changes [ZYS14]. Recent advances in 3D printing also facilitate harvesting such energy using delicate coil-magnet mechanisms that allow the resulting devices to harvest vibrations of minute magnitude that were beyond previously possible [KSL20, CR16]. Finally, such oscillations can induce a triboelectric effect that has recently been enhanced by the exploration of nano-level structures, resulting in sensing systems that could be powered by sound, the very signal they aim to sense [AZS18, AA18, Lin14]. Less common are microbial fuel cells (MFC), which have also shown promise in prior work in powering sensing systems [MGL10, MP22].

To generalize energy harvesting to a wider set of use cases, prior research has investigated general-purpose platforms and pipelines. For example, Campbell and Dutta [CD14] proposed a pioneering generic system architecture that runs on energy scavenged from environments to detect events in buildings. The difference between signals that yield energy and signals that need to be sensed often means separations between energy harvesters and sensors. In

the HVAC sensing example shown by the prior work [CD14], light energy has to be harvested from a solar cell on a window delivering energy to the airflow sensor attached to the HVAC vent through a long wire. This configuration might be obtrusive to user environments and undermine the durability. To mitigate this undesirable configuration, prior work looked into energy and signal that can be bundled together. OptoSense [ZPZ20a] proposes a light-sensing pipeline that runs on energy harvested also from light, resulting in a fleet of compact and versatile sensors. In another example, Sozu [ZIJ19a] proposed a general sensing pipeline that leverages the very harvested energy as the signals for sensing, by transforming this energy into RF broadcasts.

3.2.3 People as Power

Another popular source of power comes from users themselves – people can be leveraged as major sources of energy. This creates an inviting opportunity to address the power constraints on wearable devices [SP04]. For example, the swaying motion of arms can be harvested by coil-magnet mechanism [WTZ17], and mechanical oscillations induced by foot stepping can be turned into energy using an array of piezo discs [YGJ21]. Even the seemingly minute thermal energy dissipated by human skin can be turned into electricity using Peltier junctions [PSO16]. It is also possible to combine multiple energy sources, as is shown in Facebit [CRB21], which investigated different types of energy harvested from wearers' faces, including motion, breath, and thermal, all of which can be easy to find at the proximity of masks.

Closer to MiniKers is prior work that exploited user interactions with interactive systems and objects around. First, there have been commercial products such as self-powered doorbells [Mat22] and switches [Sen22], which transmit RF broadcasts powered by energy harvested from button presses. In the research domain, The Peppermill [VH10] demonstrates a self-powered interaction paradigm. In this example, the device allows users to rotate a knob to generate power for sensing user interactions, such as button presses. Similarly, Energy-

Bugs [RSK14] harnesses electricity generated by children shaking energy harvesters with coil-magnet mechanisms. Using a different class of harvesters, Paper Generators [KPF13] allow power generation from users performing touch, tap, and rub gestures on paper leveraging the triboelectric effect. Recently, Battery-free Game Boy [DKH20] demonstrated an energy-aware gaming platform that uniquely combines energy generation with game actions like button presses. Closest to our work are previous systems that aim to harness energy resulting from user interactions with everyday objects. Among the fleet of examples, one class of devices in Sozu [ZIJ19a] turned user motion (i.e., turning mailbox flags, using pruners, opening/closing pill bottles, drawers, and doors) into RF broadcasts for sensing applications.

3.3 Design Goals

Based on our review of existing smart environment automation systems and user expectations as discussed in literature [RPS22, VSC16], we set several design goals for MiniKers, which we achieved in this research:

Rich input. Unlike personal devices, automation in environments has unique challenges to overcome because environments are often shared across multiple users, each having their unique set of capabilities and preferences. This diversity demands interactive systems in shared environments to accommodate diverse interactions. Ideally, the device should offer a wide array of interaction modalities (e.g., touch interaction, voice control) or even multimodal interactions to fit user needs. This design goal was drawn from the recent success of commercial smart environment solutions, with which users often have various controls of smart appliances like lights [Phi22], TV mounts [sol22], window shades [HOM22], and screens [Som22], using tangible buttons, remotes, apps on smartphone and tablets, or voice.

Compatibility. Practical automation techniques should consider all stakeholders in the environment. Specifically, there needs to be automation that does not compromise the functionality and ergonomics of existing objects. This design concept has been demonstrated

in literature [CKL21, DVT11, Swi22, Stu22, ZIJ19a]. In the context of this project, we aim to have compact and versatile mechanisms that can easily retrofit existing environments. Ideally, the core components (e.g., motors and gears) could be readily applicable to a variety of objects without altering their existing structures and affordances.

Adaptability. Adaptability has been a common feature in smart environment products such as smart lights, thermostats, irrigation systems, etc. that can adjust brightness, temperature, soil moisture using sensory data from the environment. Similarly, our automation system needs to have situational awareness to respond intelligently to a different system and environmental status. For example, the system should adjust intrinsic parameters (e.g., motor current) in response to different energy levels and use frequencies. We achieved this through energy awareness – enabling MiniKers to probe energy supply and consumption at key points on the circuit board. We implemented a programmable resistance in the motor powerline and PWM motor drive to adapt the motor current to the system's energy status.

Low cost and durability. Practical automation systems should be low-cost to be scalable. With a house that could easily consist of more than 20 objects to automate, the cost of instrumenting each should not exceed $50, totaling the whole house of automation with $1000, which is comparable to a middle-end smartphone or a laptop. At the same time, lowering the price tag should not be at the cost of durability. The system needs to be robust against exposure to elements (e.g., temperature, humidity, and impact). This design goal has been sought after in previous IoT systems (e.g., [ZIJ19a, AMM21, CD14]). In this chapter, we demonstrate and evaluate how MiniKers achieve these with a 48-hour deployment study on 9 objects across 3 locations of different configurations and functionalities.

3.4 System Design

3.4.1 Overview

Based on insights from the aforementioned tests, and taking into account our design goals, we implemented MiniKers system. Our system is composed of: 1) a fully self-sustaining wireless circuit board, which connects to a mechanism and a motor to capture energy and actuate; 2) a phone application to support end users with a variety of interactions to activate the actuation, as well as to keep track of all MiniKers in the environment.

3.4.2 Hardware

Overall Structure. The MiniKers custom circuit (Figure 3.1) was designed to accommodate energy characteristics found in the previous investigation studies. The circuit has two energy storage devices: a rechargeable supercapacitor and a Lithium-ion Polymer (Li-Po) battery. We used a supercapacitor which has two capacitance options (0.6 F and 2.5 F) depending on the application – among the 9 objects in Figure 3.3, only the *MiniKers* for the backdrop used a supercapacitor of 2.5 F capacitance for the significantly large amount of energy generated in each manual operation. Similar in concept to the power grid stability support for renewable sources, supercapacitors and Li-Po batteries (3.7V, 70mAh) provide stable energy storage to buffer the intermittent user-interaction energy. The Li-Po batteries can power the motor continuously for more than two hours. This deep energy reservoir makes the system more tolerant to short energy consumption surge, improving the overall system's power reliability.

The circuit features a discharging and a charging mode to support the motor being used as either an actuator or a generator. Figure 3.2 shows the power architecture of MiniKers which accommodates the coexistence of these two modes on the motor front end. In the discharging mode, the motor is driven by a motor driver, drawing power from the battery.

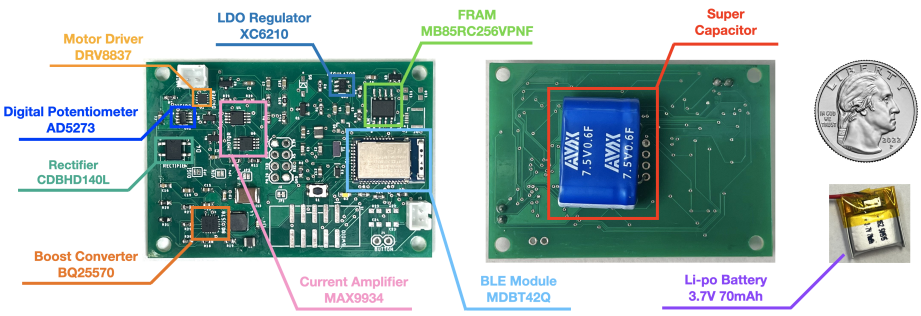

Figure 3.1: MiniKers circuit board (front and back).

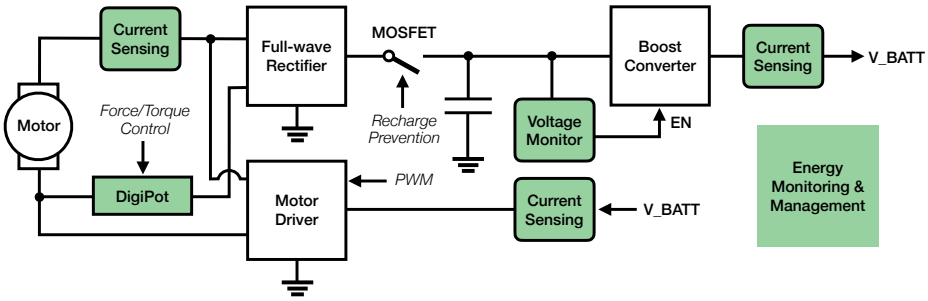

Figure 3.2: The power architecture of MiniKers.

A MOSFET is used to disconnect the charging line in this mode. In the charging mode, the motor is driven by user interactions and generates currents, which are regulated by a bridge rectifier and immediately stored in a supercapacitor. Once the voltage of the supercapacitor reaches a certain threshold, the boost converter starts working and feeding energy into the battery.

In addition, our circuit features an FRAM to store energy-related information (i.e., the voltage of the battery, energy charged into the battery, and energy consumed by the motor and the rest of the circuit) and time-related information (i.e., timestamps of charging, events of manual and automatic operations). We used a digital potentiometer (DigiPot) in the motor powerline to adjust forces/torques required in users' manual operations of objects. This DigiPot was disabled in automatic operations. In total, our board costs $45 to make as a one-off prototype and could be even cheaper in bulk productions.

Energy-Efficient Implementation. We optimize the energy efficiency of our system on two fronts: lowering power consumption and increasing harvested energy.

Our boards use a Nordic nRF52832 SoC packaged with Raytac's MDBT42Q BLE module, which features ultra-low idle-mode power consumption (less than 2 µA [Nor22]). We implemented two standby modes depending on if BLE connectivity is required. The BLE connectivity allows MiniKers to hitchhike existing interactions on smartphones using our phone apps. When users are expected to control MiniKers with smartphone interactions, BLE connectivity should be readily available and thus our system should maintain a periodical BLE advertising (i.e., first standby mode). To reduce power consumption, we tuned advertising parameters, including TX power (0 dBm), advertising interval (318 ms), and period (5 s). We also implemented a second standby mode which does not require BLE connectivity but uses event triggers on GPIOs (i.e., hardware interrupt) that monitor physical interactors such as buttons. We will describe the phone apps and interactions our system supports later in this chapter (Section 3.4.5).

Other than the SoC, the rest of components are also low-power to minimize the current draw of the whole circuit (e.g., motor driver: Iq=30 nA, boost converter: Iq=5 nA). We also configured GPIO pins to be in high-impedance mode when they are idle. To further reduce power consumption, we used power gates by adding multiple high-side p-channel MOSFET as power switches to shut off major components including current amplifiers, FRAM, and DigiPot when they are not in use.

Additionally, we configured a GPIO to capture hardware interrupts triggered by the motor in the generator mode (i.e., actuated by user interactions) to turn on high-speed ADC (at 10 FPS). This allows us to preserve the sensing resolution without losing much energy on ADC in the standby mode when no user interaction happens.

We also found large stall currents that occur at the ends of object motions (e.g., drawer fully closed/opened) when the motor is stuck. To shorten durations of the stall current to preserve energy, we implemented stall current detection using thresholding (i.e., stall current

is often significantly larger than ordinary motor driving current) and cut off power to the motor immediately once the stall current is detected.

Finally, we implemented features to increase the efficiency of energy harvesting. We used a low-forward-voltage rectifier, the output of which goes immediately to a supercapacitor (i.e., the storage capacitor), which has high pulse power capability, capturing as much energy as possible from the motor. Our system turns on the boost converter only when the voltage across the storage capacitor exceeds 2 V, forcing the boost converter to operate in the *boost mode* which has the highest converting efficiency.

Energy as Sensory Feed. Our system monitors the harvested and consumed energy which can serve as sensory feeds needed in smart environment applications. Two current amplifiers are leveraged to sense bi-directional currents through the motor and battery. The voltage level of the supercapacitor and battery are measured with analog pins on the SoC. By monitoring the energy flow, MiniKers keep track of the battery level and adapt the resistance in the motor powerline to keep them self-sustaining. Specifically, our system could increase the harvested energy per manual operation by decreasing the resistance of the DigiPot. If self-sustaining is not feasible (i.e., there are more automatic operations than what the energy harvested from manual operations can sustain), MiniKers' energy monitoring capability could be used to request user intervention (e.g., charge/exchange batteries, add other types of harvesters) as opposed to doing nothing and letting the battery drain out, which could result in unexpected failures that lead to costly errors.

Without having to use external sensors to probe user and environmental context, our system can yield quite significant amount of information by observing the energy pattern. For example, rich information can be inferred by sensing the magnitude and direction of the motor-induced current, which correlates with the motor status. For example, the current direction of the motor on a door *MiniKers* indicates whether the door is being closed or opened. We will show more sensing modalities in section 3.5.

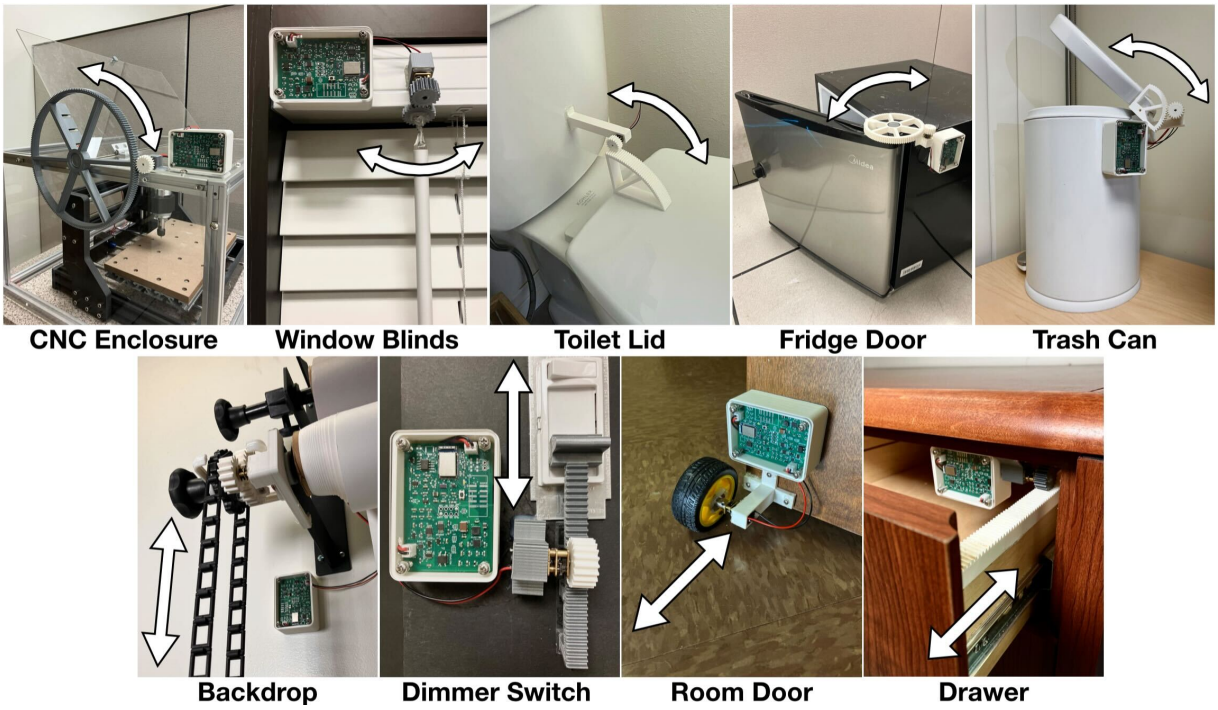

Figure 3.3: MiniKers instrumented on 9 everyday objects, enabling self-sustaining automatic operations. Top row shows objects with rotational movements and bottom row with translational movements.

3.4.3 Gear Mechanisms

We designed 9 two-gear mechanisms with unique variations to adapt to objects across a multitude of environments. These mechanisms provide additional gear ratios to facilitate our motors to actuate objects. We designed these mechanisms to function in a bi-directional manner in the sense that input and output gears could alter their roles according to the two different modes of system operation (i.e., manual and automatic). We used an Ultimaker S5 3D printer to print these gear mechanisms with PLA of 100% infills. We resolved the following challenges by fine-tuning the mechanical parameters (i.e., module, gear ratio, pivot axis, material infill, and locations relative to the host objects) of the gear:

- The additional force caused by the gear mechanisms in concert with the motors should

not be too large for a user to manually operate objects.

- Sufficient force could be provided to actuate objects (many of which could be heavy) when these mechanisms are put in a reverse configuration.
- For objects with translational motions (e.g., drawers), the mounting height of the pinion with respect to the rack has to be precisely adjusted to avoid additional force/torque due to friction while maintaining robust couplings between the two.
- For objects with rotational motions (e.g., toilet lid), the mechanisms have to be precisely mounted on the axes, or the gears would either jam or lose contact.

3.4.4 Phone App

To facilitate the use of MiniKers, we implemented two phone apps: one that allows users to control devices (the "control app"), and one that allows building maintenance and facility to review historical usage data (the "management app"). The control app displays the BLE devices that are in range, filtering out non-*MiniKers* devices using custom UUIDs. It allows users to connect to MiniKers and control them remotely with interactions available on the phone. Besides touch interactions, the control app also supports voice commands. To start, the user presses a button, then speaks a command, such as "open door". Upon each connection with MiniKers, both the control app and the management app retrieve unread data from the device FRAM. This data includes key timestamps of events, battery voltages, motor-related currents, and actuation type (automatic or manual). It is then stored in an SQLite database and uploaded to the app-specific folder under the user's Dropbox account as a proof-of-concept implementation of cloud storage.

The management app downloads the database from the server during launches and allows users to select a device to view its historical data. After selecting a device in the management app, the user is taken to a calendar view, which displays colored dots on each date to indicate automatic and manual usage with orange denoting automatic operations and green manual

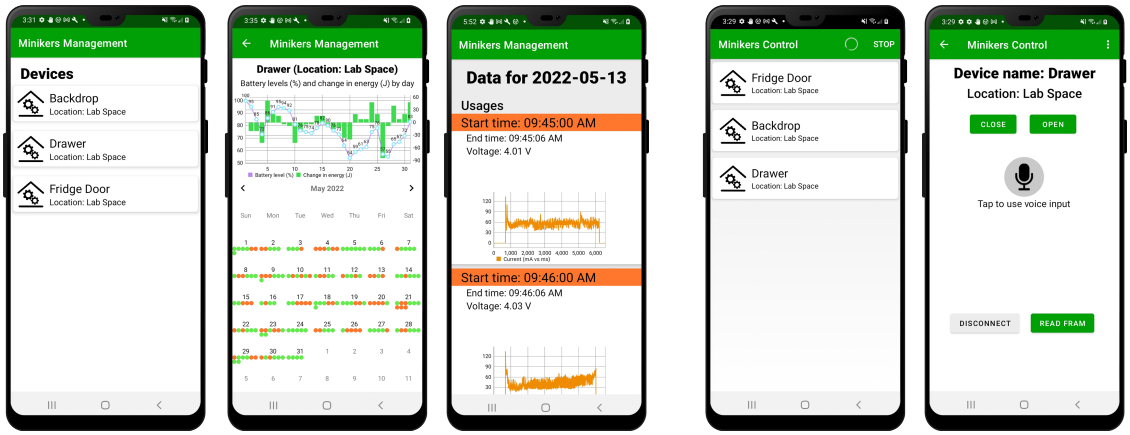

Figure 3.4: Left: the data management app (homepage, calendar view, and single day data display); Right: the control app (Bluetooth scan and control).

operations. This allows users to observe general usage trends at a glance, e.g., on which days a device was used and roughly how often automatic operations occurred compared to manual ones. From the calendar page, the user can tap on a day to view its detailed data.

3.4.5 Interaction Modalities

MiniKers support multiple interaction modalities to accommodate for various interactions affordable in user environments. First, our systems lead out several external analogs and digital pins that could be quickly turned into touch sensing mechanisms using **mechanical controls** (e.g., click, pan, twist, tilt [XLH14]) or **capacitive touch** which features thin conductive layers resulting in minimal intrusiveness to existing objects (e.g., [SZH12]). Second, these spared pins and interface bus (i.e., SPI and I2C) we led out can interface MiniKers with **external sensors** such as proximity, motion/occupancy, gesture, pressure, heat, humidity, CO2, vibration/acoustics sensors, for additional sensing capabilities. Additionally, our phone apps extend the interaction modality of MiniKers. Users could use **touchscreen interactions** to control MiniKers. We also implemented **voice control**, a commonly used interaction modality to assist users with limited upper extremity mobility [PRC19]. Finally,

MiniKers support **assisted actuation**, with which our system senses initiations of user manual operations of objects and actuates these objects to complete the rest of the operations, a common feature on automatic doors.

3.5 Validation

We validated MiniKers with a series of micro-benchmark tests described here. Results from these tests outline our system's performance envelope such as power consumption, motor actuation, and harvesting efficiency. Not only do these results further our understanding of MiniKers, they also provide benchmarks for future systems in similar application domains to compare with and improve upon, providing a foothold for ubiquitous self-sustaining smart environment automation research. Results in this section are validated by a deployment study which we will discuss in Section 3.6.

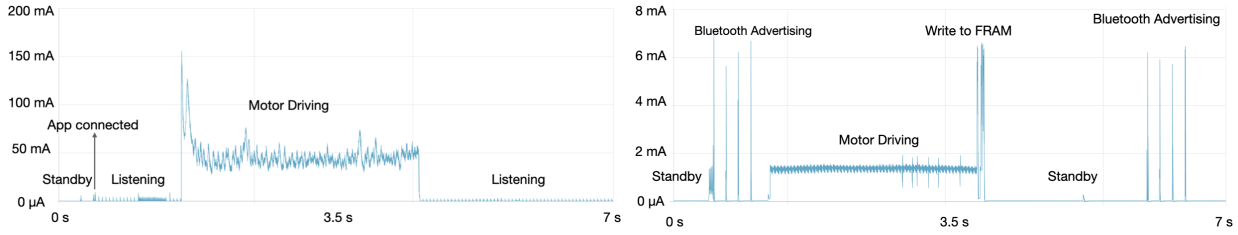

Figure 3.5: Current draw of MiniKers during a typical automatic (left) and manual (right) operation.

3.5.1 Power Consumption

Intuitively, our system consumes different amounts of power when operating under different modes for differences in power to motors, frequency of ADC, and BLE communication. We used Nordic PowerProfiler II to profile the current draw from battery of MiniKers over time in energy harvesting mode (i.e., manual operations) and actuating mode (i.e., automatic op-

erations). Figure 3.5 shows the results, with key states highlighted. Table 3.1 shows power consumption of main components. In the standby mode, MiniKers draw 45 µA from the battery. Of note that the power consumption for the standby mode runs 1) operation of the SoC and its supporting components (e.g., regulator), and 2) periodic BLE advertising. A manual operation does not involve BLE communication and has a power consumption that runs 1) ADC (hardware interrupts by motor revolutions due to user interactions), 2) boost conversion, 3) writes to FRAM, 4) current measurement, in addition to 5) the SoC operation. The automatic operation consumes power for 1) powering the motor driver that drives the motor, 2) BLE communication with the phone app, 3) writing to FRAM, 4) current measurement, as well as 5) the SoC operation. We found an average power consumption of 26.6 mJ per transmission of one Kilobyte through BLE with our system. Of note that the power consumption of enabling the activation of automation (i.e., accommodating the aforementioned user interactions) is negligible for touchscreen interactions and voice control hitchhiking existing BLE communications, and other interaction modalities (e.g., mechanical controls, assisted actuation) implemented with hardware interrupt. Accommodating interactions based on external sensors and capacitive touch could consume more power but both can be implemented in a low-power manner by careful part and frequency/duty-cycle selections.

3.5.2 Energy as Sensory Feed

The mere presence of energy can often serve as sufficient sensory feed. In fact, repurposing energy as sensory feeds has been shown in several previous works [DCD13, CD14, ZIJ19a]. In the context of this research, for example, there will have to be generated energy when a door panel is in motion, and thus sensing the presence of the generated energy can reveal uses of the door. Even better, motor mechanisms yield currents that constitute the energy flow, revealing richer signals of motions – e.g., speed, duration, and direction. And thus by sensing harvested energy through sensing currents, we can infer much about user environments

Table 3.1: A breakdown of power consumed by major components (ones labeled PG are power gated). Measurements were collected when power gates were switched on and when these components are enabled.

Component (part number)	Power (µW)
Motor driver (DRV8837)	1584.6
Current amplifier (MAX9934)	2416.8 (PG)
SoC Mininum System	148.5
FRAM (MB85RC256VPNF)	33 (PG)
DigiPot (AD5273)	3.66 (PG)
Boost converter (BQ25570)	3.8

without external sensors.

We used MiniKers system's current sensing to measure current outputs by several objects and compare them with the Nordic Power Profiler II. Figure 3.6 shows the results which indicate a modest difference between these two sets of measurements though the noise floor of our built-in current sensing is higher. We used a room door as an example to demonstrate the sensing ability of MiniKers (Figure 3.7). We used our built-in current sensing to measure current outputs by objects in their manual operations. Uses of doors indicate utilization rates of environments, and the states of doors often have social meanings – an opened door vs. a closed door. Rich sensing is needed and has been researched in prior work [YT10, SKT16, ZIJ19a, ZPZ20a], and there have been commercialization efforts focusing on door sensing [Mob22, Aut22]. In the context of room doors, our system detects what angle does the door open to (Figure 3.7 left); at what speed (Figure 3.7 middle); and in which direction (Figure 3.7 right), all of which are achieved through repurposing the motor as a sensor and leveraging the harvested energy as sensory feed.

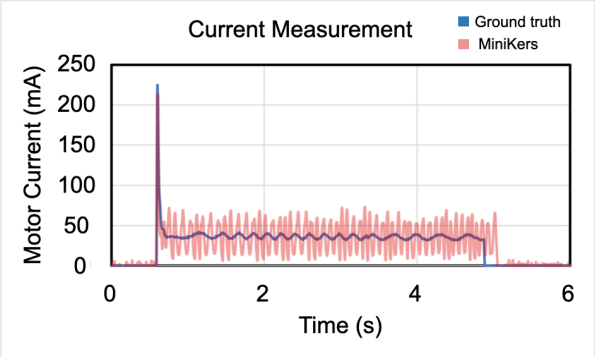

Figure 3.6: Comparison of current measurements with MiniKers and Nordic Power Profiler II (ground truth).

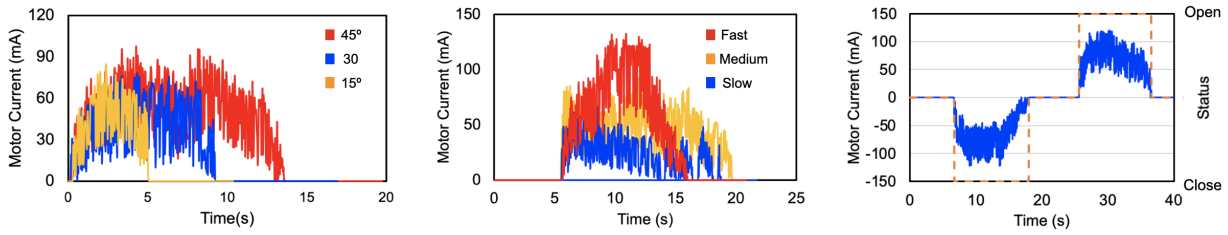

Figure 3.7: Example of using MiniKers's sensing capability. Left: The integral of motor current correlates door angle. Center: The speed of opening/closing the door can be inferred from the magnitude of current. Right: The direction of the current indicates the door status.

3.6 Deployment Study

3.6.1 Procedure

We deployed 9 MiniKers across 3 locations: a lab space, an office, and an apartment, each featuring common but different functions (Figure 3.8). These locations were occupied during the deployment and MiniKers were exposed to users and elements expected to be seen in everyday settings (e.g., humidity, pressure, impact, user interactions). Each *MiniKers* was deployed for 48 hours during which one experimenter visited these devices three times a day (i.e., morning, noon, and evening) for performing trials that were recorded for ground-truth

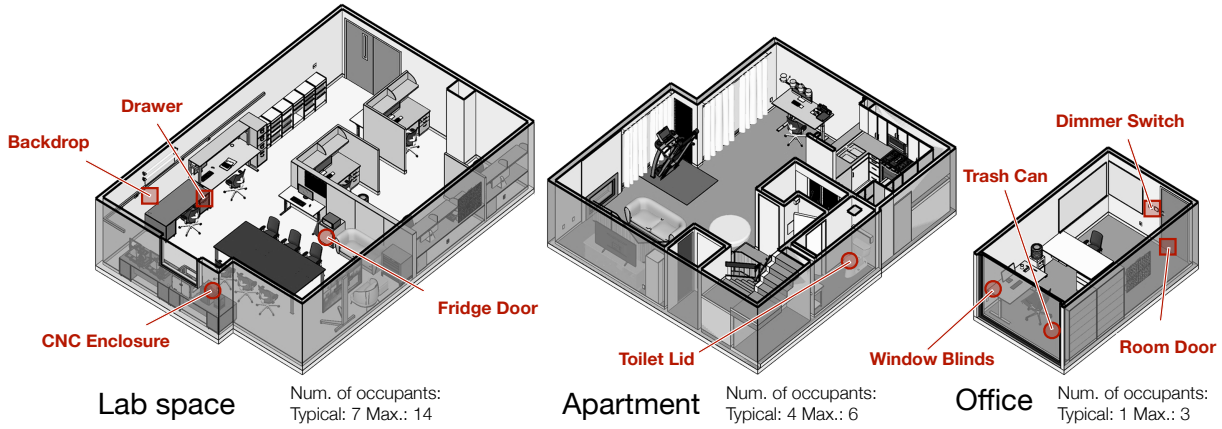

Figure 3.8: MiniKers were deployed at 3 locations on 9 objects. 3D models of these 3 locations with details of their configurations are shown. Objects with translational motions and rotational motions are denoted with squares and circles respectively.

data. Specifically, during each visit, the experimenter performed 25 manual trials of the object consecutively with a five-second interval in between, followed by 3 automatic trials using the phone app (i.e., the control app). In manual operations, the experimenter manually actuated the object from one extreme position to the other (e.g., blind blades tilted at 0^{o} for minimal light through, and at 90^{o} for maximum light through). We collected the MiniKers boards at the end of the deployment and parsed the data in the FRAM for analysis.

3.6.2 Results

Across the 3 locations and the 9 MiniKers devices, the averaged energy harvested from each manual operation was 0.26 J (SD=0.37) and the energy spent in each automatic operation was 4.46 J (SD=4.47), resulting in approximately a 24:1 ratio. In other words, there need to be around 24 manual operations of objects before MiniKers gather sufficient energy for one automatic operation. This is a rough estimation omitting several supporting functionalities (e.g., communication and system standby) that also consume power, as we have shown and quantified in the technical validation (i.e., Section 3.5). For this reason, the 24:1 ratio of

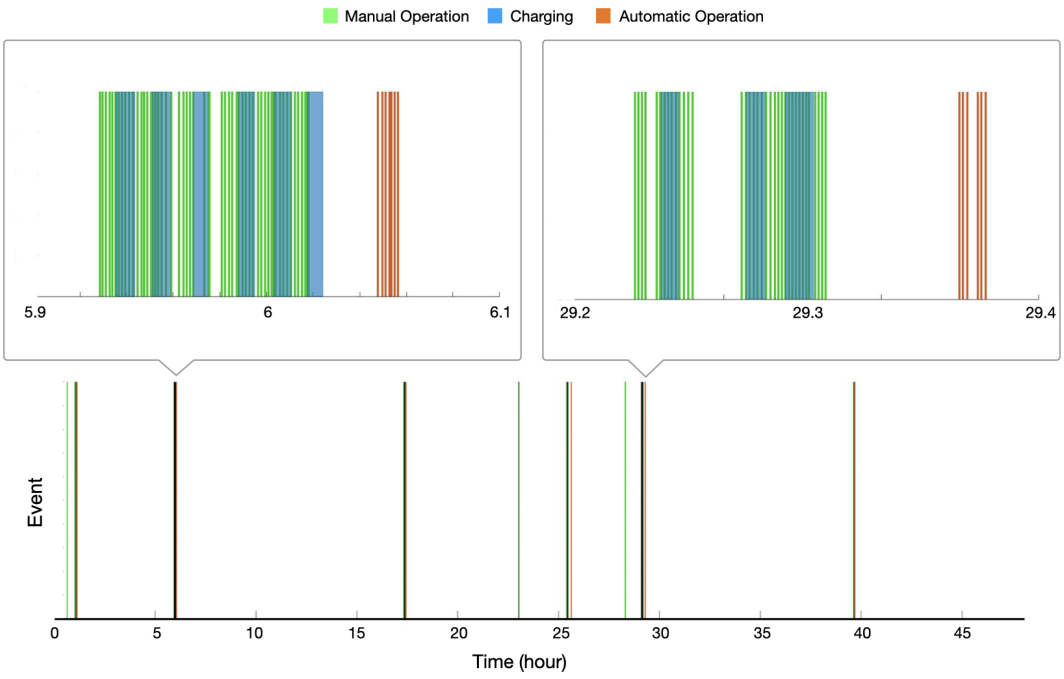

Figure 3.9: Event distribution over time of the *Fridge Door* during the deployment study. There are six periods of time in which events are concentrated due to trials performed by the experimenter. Figures on the top show two zoom-in views of these recorded events. Isolated events are due to the daily uses by owners of the space.

manual to auto operations is the upper bound of performance if MiniKers are to be deployed for real-world applications. Nonetheless, this ratio gives us an estimate, which is important in setting up user expectations and could guide users in their deployments of MiniKers in the real world. Below we break down this result into details with an in-depth analysis.

Figure 3.9 shows an example of fridge door events over time during the deployment. Table 3.2 shows harvested and consumed energy per manual and automatic operation for each object. First, we confirmed the observation from our validation test that more energy can be harvested from objects with longer motion strokes (either translational or rotational). Heavier objects (e.g., room door, toilet lid) consumed more power to actuate. In general, objects that drew more power for actuation generated more power in their manual operations.

Despite this correlation between the amounts of consumed and harvested energy, the manual-to-auto ratio still varied a lot across different objects, possible reasons for which could be differences in objects' original structures. For instance, some objects like the toilet lid have higher frictions to be actuated due to the anti-slam mechanism than others. There is also variation introduced by our gear mechanisms that could contribute to the variation of the manual-to-auto ratio.

Table 3.2: Average energy harvested and consumed per manual and automatic operation by the 9 objects.

Object	Harvested Energy (J) per Operation	Consumed Energy (J) per Actuation	Manual-to -Auto Ratio	Energy Efficiency
Room Door	0.26	10.34	40	65%
Trash Can	0.06	1.01	17	57%
Window Blinds	0.09	2.60	28	34%
Dimmer Switch	0.03	0.40	14	45%
Drawer	0.31	2.03	7	68%
Backdrop	1.22	13.32	11	81%
CNC Enclosure	0.18	1.98	11	80%
Fridge Door	0.07	3.03	43	37%
Toilet Lid	0.12	5.41	45	48%
Average (SD)	0.26 (0.37)	4.46 (4.47)	24 (15)	57% (18)

Finally, with our board's current sensing capability, we can readily measure energy efficiency by measuring and comparing the energy generated by the motor and charged into the battery. The efficiency is computed as a ratio between the two. We estimate the energy generated by the motor by monitoring the voltage increase on the supercapacitor. Energy dissipated on the rectifier and DigiPot is relatively small and thus neglected in this calculation. On average, we found an energy efficiency of 57% (SD=18). Table 3.2 shows a

breakdown of this efficiency across all objects. Like the manual-to-auto ratio, this energy efficiency also varied by object for the same reasons as previously mentioned.

3.7 Discussion

Ultra-Low-Power Standby Mode. We found a non-negligible amount of energy consumed by MiniKers in their standby mode during the deployment study. This energy outlet is going to be even more significant in longer-term deployments (e.g., year-round). This power consumption can be lowered (i.e., from 148.5 to 108.9 µW) if controls are not mediated through BLE connectivity but with physical interactors (e.g., buttons), which are common to find on existing automatic devices – automatic doors in most commercial buildings would simply use a button as a tangible and readily available interactor for control. It is also possible to choose microcontrollers with lower power consumption for e.g., the TI MSP430 series, which have shown promise in many previous energy-constrained computing systems.

Gear Mechanism Installation. Installing gear mechanisms onto objects with rotational motions (e.g., fridge door, toilet lid) poses a real challenge. These mechanisms must be precisely mounted on the object's axis of rotation, or the MiniKers gear transmission will either jam (gears being too tight that creates unnecessary friction making them hard to actuate and easy to wear) or lose contact (gears being too lose that creates backlash, skipping teeth during its rotation). This rotation axis is intrinsic to objects once they are manufactured. Thus, pinpointing their axes of rotations can only rely on a trial and error approach and could be laborious. Additionally, some objects might not be properly leveled against their surroundings and require further adjustments to our mechanical design.

Cope with Intermittency. The current implementation of MiniKers does not provide mechanisms for recovering computational state after a power failure. Significant work has been done in the area of "intermittent computing" [HS17] where energy harvesting and

battery-free devices will frequently die when energy is not available, then reboot and restore the previous computational state: examples include the Battery-free Game Boy [DKH20] which allowed for power failures without changing game state. Using the small Li-Po battery as a rechargeable energy reservoir improves power stability for our design and allows us to explore the ideas around these user-powered items without the added complexities of intermittency. However, future work could pursue full-stack implementations of intermittent computing to enable a much longer lifetime and battery-free, perpetual operation of MiniKers in more real-world use scenarios.

Usability and User Behavior. MiniKers were deployed in common everyday environments in which occupants used the instrumented objects as they normally would during the development. The system worked well with only a few breaking parts which could be improved with superior fabrication techniques (e.g., metal printing) and more permanent attachments (e.g., screws). We didn't notice any difficulties of using these objects in manual or automatic operations except for minor issues such as slow actuating speed, and long Bluetooth scanning time. Though falling out of the scope of our core research contribution, the lack of a systematic usability study is one of the limitations of this project. The usability of MiniKers should be properly investigated in our future work, including studies on populations with different motor capabilities, frequency of uses in different environments and applications, and beyond. This investigation will further our understanding of user behavior in response to enhancements of their environments with automation. Having an option of automatic operation might alter people's behavior when for e.g., automatic operations are considered more sanitary and thus preferable than manual operations that require contact. Furthermore, future research will investigate how to improve users' awareness of energy using for e.g., ambient displays that communicate to users the availability of automatic operations and alert facility when systems need interventions after recognizing that self-sustaining is impossible (e.g., the demand for automatic operations is too high).

Long-Term Deployment. While results from this work show promise, we are cautious

that long-term deployments might reveal insights beyond the scope of this work but are still valuable for improving the practicality of our proposed people-as-power technique in the real world. To fully investigate this, we plan to deploy MiniKers for longer terms at our campus (i.e., year-round) and look for opportunities to collaborate with owners of public spaces such as shops, grocery stores, and restaurants for deployments in spaces of a wider spectrum of uses.

Intrusiveness. Though we did not optimize MiniKers for size, it is possible to use superior fabrication techniques to have gear mechanisms with smaller sizes while maintaining the same gear ratios. Smaller gear mechanisms require finer teeth and therefore stronger materials, which can be achieved with metallic materials using casting, milling, or DMLS 3D printing. It is also possible to use motors with higher torques and thus can drive objects without external gear mechanisms. This correspondingly requires better driving capabilities from our circuit, which we plan to investigate in the future.

Multiple Energy Sources. Though we center MiniKers around the concept of people-as-power with the sole energy source being user interactions, it is possible and should be even more practical, to utilize multiple energy sources in the real world. For example, solar cells, triboelectric nanogenerators, piezo, and Peltier junctions can be added to MiniKers as secondary energy sources.

CHAPTER 4

Interaction-Powered Backscatters for Smart Environment Sensing

4.1 Introduction

In Chapter 3, we investigated the use of interaction power for IoT actuation. In this chapter, our focus shifts towards employing interaction power for IoT sensing. Detection of occurrences or changes in events, such as human activities, object statuses, and environmental conditions, offers powerful insights about physical and social contexts, enabling computers in the environment to respond or anticipate to users' needs. Recognizing these events has long been of great interest to researchers. One straightforward approach is to equip sensors onto users or objects and examine unique signals resulted from activities of interest [LXH16, LH19, BPP09a]. However, there exist challenges in massively deploying these sensors in the environment due to their reliance on batteries which often necessitate frequent maintenance. Other approaches include remote sensors that detect signals traveling through spaces, such as WiFi [LLL18, MGD22, TZW19], sound [AYT21], vibration [SCZ20], and light [INR16, FAL19] to infer event changes in the environment. However, these approaches usually rely on complicated learning-based inference techniques to leverage the implicit signal features, and are only capable of detecting a coarsely predefined set of activities, which limits their practicality due to the high diversity and granularity of activities in the environment.

All of the above factors hinder the large-scale implementation of sensors for smart environment sensing, prompting this research to explore alternative methods. Upon examining

various activities and events in the environment, we observed that the occurrence of an activity usually involves physical movements of objects that users interact with. Prior research has been able to detect the presence of activities by the installation of tagging mechanisms that can be triggered by motions of objects. In a pioneering research, Mechanobeat [TKF20] first introduced interaction-powered harmonic oscillation tagging mechanisms to highlight the use of objects' physical movement for activity recognition. However, only presence of activities can be detected while fine-grained information such as motion direction and speed is missing. This fine-grained information often constitutes an important contextual clue which is critical for smart devices to make better inferences about their users and surrounding environments.

We are inspired to expand the sensing capability by transforming movements of objects into encoded RF responses, from which fine-grained information about users and environments can be extracted using a millimeter wave radar from centralized sensor locations such as a smart light bulb on the ceiling or smart speakers on a countertop. Millimeter wave radar, typically used in automobile and security applications, has recently drawn the attention of researchers in HCI for its potential to be integrated into smart devices such as speakers, light bulbs, and thermostats to localize users and enable gestural input [LGK16, HLG21]. Specifically, we explored using 3D printed corner reflector mechanisms to encode user interactions with everyday objects. These mechanisms do not rely on electronics or batteries, and can retrofit to a wide variety of everyday objects hitchhiking their inherent mechanical structures (e.g., gears, hinges, tracks). By decoding radar responses, fine-grained activity characteristics such as state, direction, rate, and usage can be inferred. We investigated effective corner reflector mechanism designs and developed the corresponding detection algorithm based on first-principle signal analysis. We demonstrated our system with 15 everyday objects (Figure 4.4) in indoor and outdoor environments.

4.2 Related Work

4.2.1 Activity and Event Detection

Prior works detect occurrences of events that generate different types of signals, including visible light [ZPZ20b, KFA19], vibration [ZLH18, SCZ20], RF broadcasts [LYS15, BPP09b, WLC21], acoustic signals [AYT21, LXH16], electromagnetic interference (EMI) [GRP10, CGL15, ZYH18] and air pressure [WPM15, PRA08]. In terms of sensor locations, researchers have developed wearable sensors to detect human activities [KHT21, SHK17, CGL12]. Commercially available wearable sensors have seen success in health and fitness applications (e.g., smart ring [rin23]). Alternatively, sensors can be instrumented on objects of interest such as doors, microwaves, faucets to monitor their status [ZIJ19b, ZLH18, KP10].

These sensors are often powered by batteries, making their inevitable maintenance a significant cost of deploying them in the long run. To eliminate the reliance on batteries, researchers turned to develop self-powered sensors and systems that can harvest energy from environments [ZIJ19b, ZPZ20b, GPW18] or from people [YSX22, CRB21] to supply the power for sensing. Another approach to addressing power issue is to design sensors that contains no electronics and leverages material properties (i.e., type, geometry, motion pattern) for passive sensing [TKF20, ICG17, LCY19, JWY18], with which our research shares the same scope.

4.2.2 RF Sensing in HCI

Radio Frequency (RF) sensing has long been sought after, with a majority of work focusing on the microwave range (e.g., WiFi, 2.4-5 GHz) [ZWX19, WZW16] and millimeter wave range (30-300 GHz) [LGK16, WLC21, SSG19]. Operating at these special frequencies, RF signals enables high-fidelity sensing while preserving their innate advantages of being non-contact and not constrained by lighting conditions [ZZX22, ZLA18].

RF sensing has been used in a wide array of applications including communications [NQZ21, QYZ22], user identification and localization [SPB21]. Other sensing modalities of prior works center around human activity recognition such as posture detection [KXY22, ZLA18], fall detection [WWN16], vital signal [YPZ16, WZW21], eating behavior [XJG22] and sleeping posture monitoring [YPZ17]. RF signals has also been used for sensing environmental facets such as sound [OWW21], humidity [DHW18], temperature[CLL20], material [WZW20, YFS16], and vibration [JGH20].

The recent development of compact and solid-state millimeter wave radars such as Google Soli [LGK16] opens up opportunities to enable interactive sensing such as hand gestures recognition [HLG21], tangible interaction sensing [GHP22], and interactive controls [YZ21, HWW21]. Our system builds upon this growing interest but differs by shifting its focus from sensing human to sensing objects.

4.3 Sensing Principle

4.3.1 FMCW Radar

Millimeter wave (mmWave) radar, has drawn attention from researchers in HCI due to its potential to enable a wide array of sensing modalities with a compact sensor form factor and limited privacy implications. At a frequency as high as 77 GHz, mmWave signals are less affected by interference from other sources such as Wi-Fi and Bluetooth signals, making it applicable for both indoor and outdoor environments. Radars can reveal rich information of targets including range and velocity, and those with beamforming capabilities can even sense multiple concurrent activities on targets scattered throughout the environment. Though radars are not as high-resolution as cameras, they can still yield sufficient information about targets such as shapes, deformation, posture changes for activity detection.

Radars that feature mmWave are usually modulated with Frequency Modulated Continuous Wave (FMCW) technology, which has been documented in prior work [LGK16, HLG21,

ZZX22] and will not be detailed in this thesis. In short, FMCW radar emits signals with linearly varying frequency, called chirps, and gets range and velocity of the target by measuring frequency and phase shift of the reflected signals. This chirp mechanism allows the detection of tiny displacement within a short duration (μs level), which is ideal for sensing moving objects. Besides, the power of received signals in a radar system with transmission power P_t, transmitter gain G_t, receiver gain G_r and wavelength λ, measured by Equation 4.1 [qua23], depends on the distance D between radar and the target, specifically its radar cross section (RCS) σ of the target and a loss factor L.

$$P_r = \frac{P_t G_t G_r \lambda^2 \sigma}{(4\pi)^3 D^4 L} \tag{4.1}$$

Though the reflectivity of a target (i.e., its RCS) is not the only factor that affect the magnitude of received signals, we found in practice that it is the dominant signal that explains the variance of received signals in the case of objects deployed in the environment. This is the main sensing principle we leverage in this thesis – correlating the power of received signal with the RCS change of a target. Of note that the innate reflectivity changes of objects due to their movements in response to user interactions are modest, ambiguous, and heavily affected by variances in user motions, and thus we designed reflector mechanisms to encode these movements to facilitate their detection.

4.3.2 RF Reflector

RF reflectors are conventionally used to enhance RF reflections. They have been used for communication [NQZ21], localization [SPB21], redirection [QYZ22], along with many novel use cases in research (e.g., CubeSense [YZ21]). RF reflectors can be as simple as a flat metal sheet which appears as "a mirror" to incident waves. Leveraging the rapid development of wireless technologies such as Wi-Fi and radar, recent research has innovated reflectors with unique shapes, structures and materials that allow specific control of signal propagation,

such as metasurfaces [QYZ22, ADT17], 3D-fabricated reflectors [XCY17], frequency selective surface (FSS) reflectors [JSE20].

Retro-reflectors are a common type of RF reflectors that reflect RF waves back to their source. Van Atta array is a common retro-reflector that uses conductive antenna pairs with strategically designed lengths on planar surfaces to adjust the phase of incoming RF signals [SPB21]. Corner reflectors, commonly made up of three mutually perpendicular plates, are often used in radar systems for detection [Doe14, ZZK18] and calibration [GVL90]. Incident waves undergo multiple reflections within the "corner" and eventually reflected back to their sources. Note that this redirection of waves can happen only when incident waves land on certain areas of a corner reflector, denoted by effective aperture area A_{eff}. The effective aperture decides RCS, which describes the reflectivity of a corner reflector and is estimated by Equation 4.2, where λ is wavelength and R is the reflection coefficient derived from Fresnel equation [Eck71, equ23, ref23].

$$\sigma = 4\pi R A_{eff}^2/\lambda^2 \tag{4.2}$$

This equation shows three following factors that can change the magnitude of RCS, which we considered in the design of reflector mechanisms that encode user interactions into RCS changes. We selected corner reflectors to implement our reflector mechanisms for their following merits:

(1) They offer a relatively large RCS compared to their size, leading to a high Signal-to-Noise Ratio (SNR) and consequently improved detection capabilities.

(2) They provide wide-angle reflection, making them suitable for applications involving moving objects or unpredictable radar locations in the environment.

(3) Their RCS can be described mathematically, enabling the computational design of reflectors through first-principle approaches.

(4) Their simple structure and passive operation ensure durability, affordability, and ease

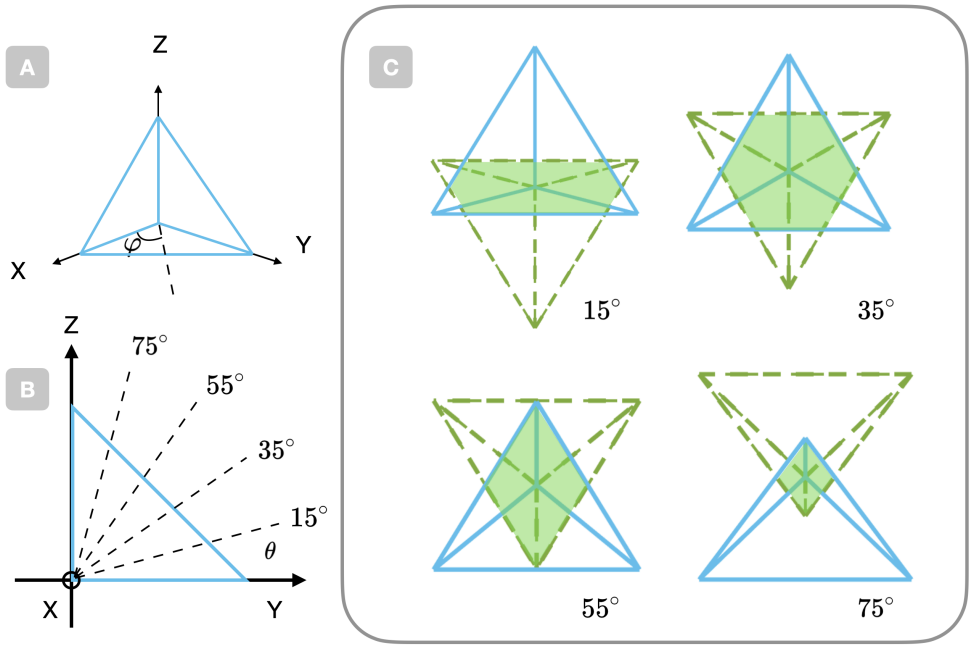

Figure 4.1: A: Front view of a triangular corner reflector. φ is the Azimuth angle. B: Side view of the reflector. θ is the Elevation angle. C: Effective aperture area (highlighted in green) with an incident angle of $\varphi = 45°$, $\theta = 15°, 35°, 55°, 75°$.

of manufacture.

Factor 1: Material Interface materials can affect magnitude of reflected waves due to the difference in electrical properties, which can be measured in Equation 4.3 by the reflection coefficient:

$$R = \left| \frac{-\varepsilon_r \cos\theta_i + \sqrt{\varepsilon_r - \sin^2\theta_i}}{\varepsilon_r \cos\theta_i + \sqrt{\varepsilon_r - \sin^2\theta_i}} \right|^2 \tag{4.3}$$

where θ_i is the incident angle, and ε_r is the relative complex permittivity of a material given by $\varepsilon_r = \varepsilon' - j\frac{\sigma}{2\pi f \varepsilon_0}$ with the real part associated with degree of polarization of a material and the imaginary part the dielectric loss, σ is conductivity of the material, ε_0 is the vacuum permittivity, and f is the frequency of RF waves [equ23]. At radio frequencies, conductive

materials such as metals exhibit a dominant imaginary part in their relative permittivity ε_r due to their high conductivity, which leads to higher reflectivity of radio waves [per23]. Dielectric materials such as plastic, however, absorb radio waves due to lack of free electrons to radiate incoming signals as opposed to metals, and thus result in greater loss and smaller RCS [BPB19]. In practice, we found that material is not an effective factor for tuning RCS because of the limited dynamic range resulted from common materials (e.g., plastic and metal).

Factor 2: Orientation A_{eff} is orientation-dependent and can be calculated as intersection between the open aperture and an inverted image aperture of corner reflector using geometric optics model [Eck71]. Figure 4.1 shows an example of aperture area varying as the angle of the incident RF signal changes. To verify RCS changes with orientation, we ran a simulation with CST studio [CST23]. Specifically, we modeled a square corner reflector made of 5 cm perfect-electric-conductor (PEC) and swept both azimuth and elevation around 0-90°. Figure 4.2 A shows the simulated radiation pattern in 3D space. There are three side lobes besides the main lobe due to reflection on the three unit plates when the incident waves land perpendicular to them. This is aligned with the signal pattern we measured in the real world which we will discuss in Section 4.4.

Factor 3: Geometry Geometry includes the *shape* as well as the *size* of the unit plate on a corner reflector. Common shapes of a unit plate include triangular, circular and square. With the same shape, RCS varies with the edge length a, which decides the size of the unit plate and that of the overall corner reflector. Prior work has also proven $\sigma(a) \propto a^4$ at boresight [Eck71, DB09, Doe14]. To verify the correlation of RCS with a, we ran simulations for corner reflectors of 1-5 cm (at an 1 cm interval) edge length, and plotted RCS along the azimuth plane (with an Elevation angle of 35°). The result is shown in Figure 4.2 B, indicating that RCS increases with a for most incident Azimuth angles (i.e., 10 - 80°).

Furthermore, among these three factors (i.e., material, orientation, and geometry) on RCS of corner reflectors, we utilized *orientation* and *geometry* to induce RCS changes.

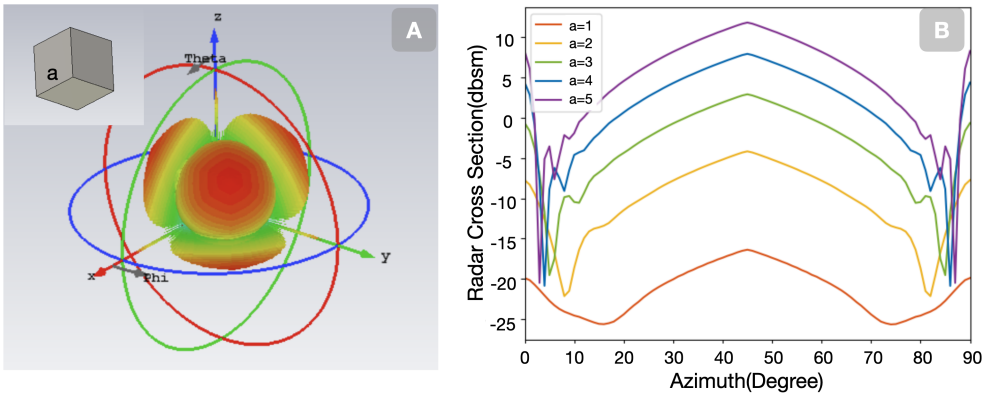

Figure 4.2: Simulation results. A: Radiation pattern of a square corner reflector (upper left: corner reflector model). B: RCS of corner reflector with different sizes ($\theta = 35°$).

Compared with these two factors, changes of *material* induce a narrower dynamic range of RCS and therefore was skipped in the implementation of our reflector mechanism. Our observation, as shown in Figure 4.2, unveils that rotations of a single corner reflector could induce RCS changes from a static radar's perspective. The rotation of one single corner induces periodic peaks of RF reflection which could reveal the status (i.e., on/off) and rate (i.e., speed and frequency) of activities. To encode richer information (e.g., direction), we concatenated multiple corner reflectors with different geometries along the periphery of a rotatory platform. The platform's rotation is driven by the movements of objects powered by user interactions through a linkage gear mechanism. Depending on the direction of rotation, the RF reflection will manifest as distinct time sequences, which can be exploited by a detection algorithm to decode directional information.

4.4 Implementation

4.4.1 Overview

Before detailing our system, we discuss some design considerations of reflector mechanisms that should be taken into account for achieving better sensing performance.

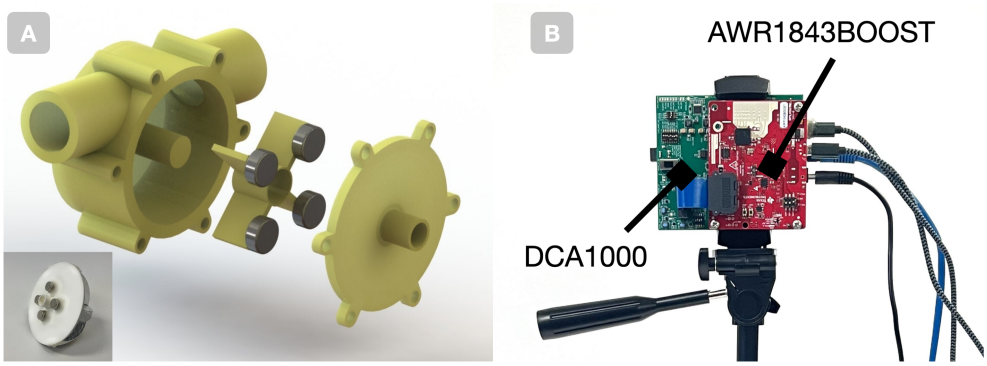

Figure 4.3: A: A pipe mechanism using magnetic coupling to enable an external rotation driven by the internal flow. The other set of magnets (shown at bottom left) is attached to the underside of the reflector. B: Radar sensor setup.

(1) The reflector mechanisms should generate signals with sufficient SNR to make it distinguishable in an environment, where stationary and dynamic objects (e.g., people and appliances in a home environment; moving cars and pedestrians in a city environment) constantly exist in the background. Strong and distinctive signals bolster the system's accuracy and reliability, ensuring its performance amid unpredictable background noise.

(2) The reflector mechanisms should encode different object status (e.g., on/off, direction, magnitude) with different signal characteristics (e.g., frequency, amplitude, phase). The difference between these signal patterns should be distinct and easy to be recognized by the radar receivers.

(3) The reflector mechanisms should be easy to fabricate, versatile to be instrumented on various host objects. They should be flexible and low-cost to deploy, and ideally have compact form factors for minimum intrusiveness.

Based on these considerations, we designed a series of electronic-free, 3D-printed reflector mechanisms for everyday objects, which can communicate with an millimeter wave radar wirelessly with rich information of their host objects. Specifically, to avoid interference of user movements, we encode speed of motions into frequency of signals, at a range much higher

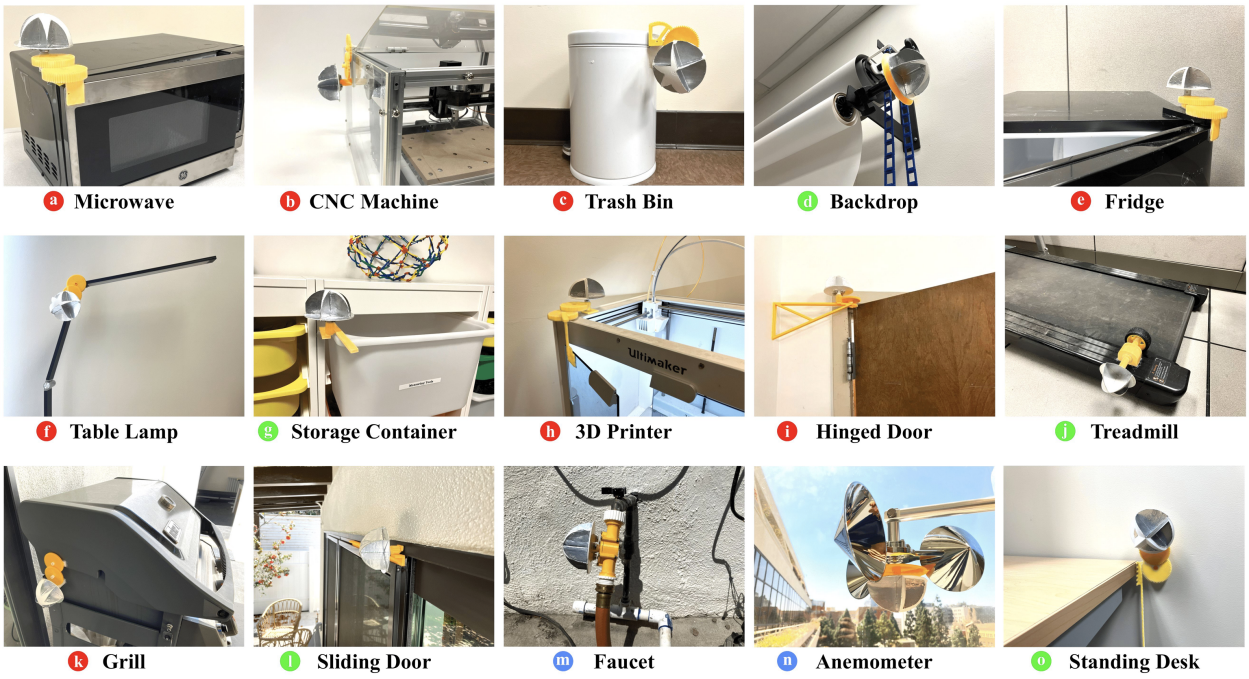

Figure 4.4: Reflector mechanisms. Red: rotational motion. Green: translational motion. Blue: flow motion.

than human body movement (e.g., 1-3 steps/s while walking, running or jumping). Gear ratios were carefully selected in designing gear mechanisms that convert user interactions (i.e., object movements) into the rotation of our reflector mechanisms.

To detect direction of movements, we encode the direction of the reflector mechanism's rotation into the slope polarity of the envelope signal containing the reflection peaks induced by corner reflectors. By changing the geometry of the corner reflector facing toward the radar through the rotation of the reflector mechanism, it exhibits a gradual increase or decrease of RCS depending on the rotation direction (i.e., clockwise vs. counter-clockwise). We adopted a computational design approach to finalize the configurations of the reflector and proved its superiority against alternative designs.

4.4.2 Reflector Mechanism

4.4.2.1 Motion Transformation

We found three common types of movements on objects deployed in the environment: translational (i.e., sliding contact), rotational (i.e., hinged contact), and flow (i.e., fluid contact). These motions can be transformed by using mechanisms to achieve a desired rotational speed of the reflector mechanism.

To ensure optimal signal quality, the rotating speed (or frequency) of our reflector, denoted as $f_{reflector}$ in revolutions per second (or Hz), must have a high value that gives its motion signal a sufficient margin against signals induced by human body motion, denoted as f_{human}, and a maximum value that does not exceed $f_{radar}/2n$, where $f_{radar}/2$ is the Nyquist frequency of the maximum frame rate threshold of the radar f_{radar}, and n is the number of reflectors in the reflector mechanism. This relationship is captured by Equation 4.4. Additionally, the reflector must revolve at least one complete turn at every trial of the activity so that the signal can exhibit a gradual change in RCS.

$$f_{human} \ll f_{reflector} < f_{radar}/2n \tag{4.4}$$

Thus, for short-stroke motions such as hinged objects, which typically operate at a quarter revolution (for opening or closing), we design a mechanism with a 1:16 gear ratio to simultaneously satisfy both criteria. This allows the transformation of rotational motion to output a valid $f_{reflector}$ by multiplying the interaction speed by 16, ensuring a high enough frequency to be discriminated from human motion while allowing the reflector mechanism to revolve 4 times in a single operation. On the other hand, for long-stroke motions such as sliding objects or continuous stroke motions such as fluid flow, we design a mechanism with a 1:1 gear ratio, which we found sufficient to yield high-SNR signals.

4.4.2.2 Magnetic Coupling

The mechanism for the flow motion of liquid running inside pipes requires a special design (Figure 4.3 A). For example, the mechanism instrumented on an outdoor faucet has one end attached to the valve and the other end to the hose. We used magnetic coupling to facilitate movement between the water wheel driven by the internal water flow and the external fixture that rotates the reflector without having gaps that often cause leakage in our early iterations. The water wheel was 3D printed with PLA. We found that the mechanism could achieve high radial movement with minimal resistance, further reducing the risk of leaks and increasing durability over time.

4.4.2.3 Reflector Geometry Design

First, we ensured the visibility of reflectors to radars at arbitrary deployment positions by having an array of corner reflectors on a hemisphere-shaped platform (i.e., a hemisphere-shaped reflector). Our reflector was designed with a hemisphere shape without sharp edges to be less intrusive to both users and environment, making it more practical in real-world applications. The corner reflectors on it ensure a wide range of workable incidence angles, allowing our reflector mechanisms to work with many radar locations (e.g., smart speakers, light bulbs).

Second, we select the approach to change reflectivity of the hemisphere-shaped reflector as it rotates. One straightforward approach is using a shield with various sizes of vents in front of a corner reflector to control the reflection of incoming signals. Specifically, we designed a cone-shaped shield with see-through vents that can rotate with gears, and a stationary corner reflector positioned inside the shield (Figure 4.5 A). We eventually abandoned this design for its delicate mechanical components, making it more challenging to set up (i.e., printing time, material consumption, and installation); and comparatively lower SNRs than the rest of the candidate designs.

We found it more feasible to leverage orientation and geometry factors discussed in Section 4.3, by concatenating multiple corner reflectors on a rotatory platform to get expected RF reflectivity pattern. In the following discussions, we use "pocket" to denote a single corner reflector on the hemisphere-shaped reflector. Our first prototype divided a hemisphere into four pockets with various sizes, and each with its edges parallel to those of its adjacent pocket (Figure 4.5 B). However, we found that it often yielded many side spikes of RF reflection, which we suspected were resulting from their unit plates when they were perpendicular to radar incident waves and from the margins between pockets. These side spikes pose challenges to our signal processing and information decoding algorithms and should be minimized, for which we decided to conduct another round of iteration.

We took a computational design approach for which we revised our design goal into: determining a concatenation of n pockets, with each pocket having an edge length of r_i, to have a monotonic RCS change across incident azimuth angles ranging from 0 to 360°. Each pocket is described by $P_i = (C_i, E_i, E_i')$ with two edge vectors $\vec{v_i}$ and $\vec{v_i}'$. Edge vectors point from centers C_i to points on the hemisphere periphery E_i (Figure 4.6 A). Of note that $E_{i+1} = E_i'$. For each incident wave $\vec{v}_I(\varphi_I \in [0, 2\pi])$, we calculate RCS of the reflector across 0 - 360° by Equation 4.5, where $u(\cdot)$ is the unit step function neglecting pockets pointing away from the radar, $rcs(\cdot)$ is derived from simulation in Section 4.3 and $\rightarrow$ is a vector projection. Specifically, RCS of a corner reflector is symmetric along the boresight (i.e., Azimuth angle = 45°, Elevation angle = 35°), so we only consider the azimuth plane on the boresight. We further assumed that only those pockets, whose two edge vectors each form an angle between 0 and 90° with the incident vector, are capable of inducing a reflection back to the radar.

$$RCS(\vec{v}_I) = \sum_{i=1}^{n} u(\vec{v_i} \cdot \vec{v}_I) u(\vec{v_i}' \cdot \vec{v}_I) rcs(r_i, \vec{v}_I \rightarrow P_i) \tag{4.5}$$

Corner reflectors, even a small one, can induce strong reflection to the radar compared to environmental noise, resulting in a "peak" of radar response as it rotates. Pockets with different edge lengths yield different "peak" characteristics, which are what we leverage to

encode information. This encoding mechanism is akin to amplitude modulation which has been widely used in communication. We define a new term to describe the hemisphere-shaped reflector that has a pocket array:

$$H = \underset{r_1, r_2, ..., r_n}{RCS}(\vec{v_I}) \tag{4.6}$$

We define peaks $(pk_1, pk_2, ...)$ induced when H rotates with certain constraints (i.e., the length of the peak array should be greater than 3) and fit them with a linear regression model using coefficients m, b and fitting error $rmse$. Then we solve the following constrained multi-objective optimization problem to find the optimal combination of pockets p_i,

$$\begin{aligned} \underset{r_1, r_2, ..., r_n}{\text{argmin}} \quad & m, -b, nrmse \\ \text{subject to} \quad & r_{min} \leq r_i \leq R, \\ & 0 \leq r_{i+1} - r_i, \\ & \sum_{i=1}^{n} \frac{2\pi r_i}{4} \leq 2\pi R. \end{aligned}$$

where $nrmse$ is the normalized fitting error, which we used to facilitate comparison between models. r_{min} is the radius of the smallest pocket bounded by environmental factors such as distance to the radar and ambient noise to ensure certain SNR (Equation 4.7). R is the radius of the hemisphere-shaped reflector. Of note that we assume that the hemisphere-shaped reflector rotates starting with the largest pocket facing the radar, and thus m needs to be as small as possible for yielding distinctive slope polarity, facilitating the direction detection. In the opposite rotation direction, m will guarantee to be the largest, assuring that one solution is optimal for both directions. We also reward a large b which is equivalent to a strong reflection when the largest pocket is facing the radar, facilitating the detection of activity presence. This optimization problem is solved by a genetic search algorithm [Cen77] in Matlab.

$$min\ r_i \propto \sigma_i \propto \frac{(SNR)P_{noise}(4\pi)^3 D^4 L}{P_t G_t G_r \lambda^2} \tag{4.7}$$

We empirically choose $n = 5, r_{min} = 1\ cm, R = 4.4\ cm$ for our reflector design, and a step of 0.2 cm for the searching space of r_i given our fabrication resolution. Figure 4.6 B shows objective function values at 18 different solutions. We selected one of the solutions by manually examining their simulated RCS patterns and picked the radius set of 4.4, 4.0, 3.6, 2.8, 2.6 cm for our design (Figure 4.6 C, D). This decision was based on design considerations such as RCS pattern including the number and magnitude of spikes, peak characteristics as well as the space efficiency of the pocket arrangement on the hemisphere. This computational design of reflectors strengthened their signal characteristic and facilitated their detection, for which we design a first-principle-based algorithm, as we will discuss in Section 4.4.4.

4.4.2.4 Reflector Material Selection

According to the discussion in Section 4.3.2, metals generally create stronger reflection than dielectric materials such as plastic, allowing more compact reflector designs that can be used in productization. We reached out to manufacturers and made reflectors out of aluminum alloy and steel with our computationally designed reflector geometry. Figure 4.7 shows results indicating that metal-printed reflectors induce strong reflection (2 - 4 times stronger than that of PLA + aluminum foil) and exhibit more distinctive signal patterns. However, metal fabrication was time- and cost-intensive due to its limited accessibility to the general public. This issue could become negligible once the fabrication of these reflectors transitions to a mass production scale. In this research, we followed a fabrication approach found effective in a prior work [YZ21] to implement our reflector mechanisms, taking advantage of 3D printing as a rapid and cost-effective fabrication approach to yield complex and customized shapes. Specifically, we first 3D-printed reflector substrates out of PLA. To enhance reflectivity, we then attached a thin, conductive aluminum foil to the pockets of the hemisphere-shaped

reflector. Our end result is low-cost, durable, and flexible to be deployed in various sizes.

4.4.3 Hardware

Our sensing system is based on TI's AWR1843 radar operating at 77-81 GHz. The sensor has three transmitters and four receivers with a 120° and 30° field of view in the Azimuth plane and Elevation plane respectively. We configured this radar to operate at a frame rate of 500 by sequentially emitting 1 chirp per transmitter per frame. We used this configuration to achieve a high frame rate of RCS sensing while being insensitive to velocity (i.e., speeds of object movement and reflector rotation) by not having multiple chirps within a frame. This is because our sensing principle is based on RCS changes rather than movements which often constitute noise (i.e., human motion) to our sensing. To ensure the separation of reflector mechanisms (∼9 cm diameter) among objects, we used a chirp configuration of bandwidth = 1.8 GHz, chirp time = 60 μs, adc samples = 256, resulting in a maximum sensing range of 22 m and a range resolution of 9.7 cm. At this resolution, multiple objects could be easily separated so long as their reflector mechanisms are not sharing the same range-azimuth bin. Specifically, we measured that signals from a reflector are attenuated by -20dB in a bounding box (i.e., a potential location for another reflector) if the bounding box is placed 29 cm, 38 cm, 45 cm apart from the reflector at 1 m, 2 m and 3 m ranges. This measurement confirmed that our radar configuration is adequate for detecting multiple objects, since many household appliances (e.g., drawer, door) are spaced more than 1 m apart. The complex (I/Q) data samples are streamed by the DCA1000EVM data capture module to a laptop over an Ethernet cable for further processing.

4.4.4 Software

The raw ADC data, stored as a stream of 256x8 matrices, is processed with FFT to obtain range-azimuth profiles, allowing us to locate reflector mechanisms in the environment. We

measure the average received power within a region of interest (ROI) over time and obtain a time sequence, to which a sliding window with 512 window length (WL) is applied to examine the signal characteristics and estimate the object status in real-time. Specifically, we used the following algorithm to determine the presence of an event, direction, speed, angle, and uses of target objects, where $Thred_{high}$ and $Thred_{low}$ are threshold values determined by host object and its environment, PW is minimum peak width used to eliminate spikes of noise. All the above parameters as well as the ranges and angles of the reflectors instrumented in the environment are obtained during system calibration. We developed an algorithm for the detection of the presence and other rich information of events, as shown in Figure 4.11.

To demonstrate the effectiveness of our algorithm, we used data collected from one instrumented object (i.e., a CNC enclosure) as an example. Figure 4.8 shows the raw signals from a single trial of opening and closing, from which we can see that the event occurrence can be segmented by applying thresholds to the frequency spectrum. Figure 4.8 C and D show detailed characteristics of the time series, wherein the envelopes of peaks from an opening trial feature a triangular wave pattern with a large peak followed by a decreasing ramp while a closing trial shows an increasing ramp followed by a sudden drop in signal magnitude. Furthermore, we collected data for different interaction scenarios including opening the CNC enclosure door at angles of 45°, 90°, 135° and 180° as well as at low, medium and high speed respectively. The results are shown in Figure 4.10, indicating the feasibility of sensing these fine-grained information about activities with our encoding mechanism and detection algorithm.

4.5 Evaluation

We deployed 14 mechanisms in two indoor environments (i.e., maker space and office) and one outdoor environment (i.e., house backyard), as shown in Figure 4.9. Details of these mechanisms can be found in Figure 4.4. Of note that we omitted the anemometer for the

difficulty of inducing its ground-truth signals in the study. At each location, the radar sensor was affixed at a certain location and went through a calibration process prior to the testing. This process included adjusting orientation, selecting a region of interest, and setting thresholds. Two experimenters conducted three rounds of testing for each object at each location. Specifically, one round of testing started with a 10-minute data collection during which objects were idle and experimenters performed daily activities such as working, talking, eating, walking, and exercising. Then, an experimenter performed 10 trials of operation on one object (i.e., one trial includes one complete opening and one closing operation) with approximately 2 seconds interval, until all objects were tested. The environments were occupied and exposed to users and elements expected to be seen in everyday settings (e.g., users walking in the maker space, windy weather in the backyard).

An example of signals from one round of testing (i.e., 10-minute data and 20 trials) for the storage container is shown in Figure 4.12. We found that signals resulting from reflector mechanisms (i.e., the thick oscillations in Figure 4.12 B and C) were much more distinctive than idle signals (i.e., signals in between oscillations). We also observed that activities involving RF reflective materials, such as opening or closing a laptop (spikes in Figure 4.12 A), had a higher chance of triggering false positive detection. This observation was common across all objects we tested in this study and validated the effectiveness of our reflector design.

Our dataset consisted of 840 trials of operation, and the results showed a low false positive rate (only 5 times out of all the 10-minute idle data collection from the 14 mechanisms, counting 7 hours in total) and a true positive rate of 98.25% for use detection. On average, direction detection accuracy was 80.2%. The table at the right side of Figure 4.9 shows the detection accuracies for each object. We found a minimum impact from the variations in environments and object locations on the detection of object use. A more significant impact was found on the detection of direction. As the distance between objects and the radar sensors increased, the direction detection accuracy decreased, for the lower SNR due to the

larger path loss of radar signals during the transmission.

4.6 Discussion

One obvious limitation is the limited sensing capability on objects out of radar's line of sight. The penetration capability of RF waves decreases with their wavelength in the GHz frequency bands assuming a constant power. However, shorter waves enable sensing with higher spatial resolutions that allow better differentiation between multiple objects in the environment as well as smaller reflector form factors. To mitigate this limitation, one possible solution is to leverage reflections of RF waves on everyday surfaces. This solution has shown promise in prior works demonstrating Non-line-of-sight (NLOS) radar sensing techniques [HTY21, WKO21, FLZ21].

Currently, reflectors are registered to locations (i.e., unique combinations of Range, Azimuth, and Elevation) of their host objects, thus necessitating a manual calibration process. However, this calibration is only required at the installation or when object location changes, which is often infrequent for many objects (e.g., facets, doors, windows). The effort required for calibration is comparable to setting up new IoT devices. Nonetheless, we recognize this as a limitation of our current approach. Sensing movable objects is unachievable through this location-based identification. Looking ahead, hybrid sensing approaches (e.g., with RFID) and advanced signal processing could potentially facilitate the identification of objects and thus eliminate the need for calibration.

Another challenge is the design of gear mechanisms that retrofit existing environments. Particularly for hinged objects, the axis of rotation is difficult to locate. We expect sensor-aided approaches using vision or IMU sensors on mobile devices to be possible, as shown in prior work [LKC19, LSK22]. Additionally, the gear mechanisms are bulky in our current design, however, smaller gearboxes exist and could be achieved with superior fabrication methods (e.g., metal printing). A long-term solution to eliminate a user's installation effort

and to minimize the reflector form factor is to integrate the reflector mechanism into the manufacture of everyday objects, or to be provided as accessories by the manufacturers as an optional enhancement (akin to the furniture wall straps).

Though we did not demonstrate concurrent activity sensing, we noted that activities that are sufficiently separated should be able to be independently detected due to the minimal interference caused by overlapping of reflection on the range-azimuth map. Nonetheless, further research is necessary to extensively explore its feasibility. Future work could utilize advanced beam-forming approaches to distinguish signals from various sources in complex environments that involve multi-path interference, as well as overcome security challenges including spoofing and MITM attacks, both of which are limitations of our sensing approach.

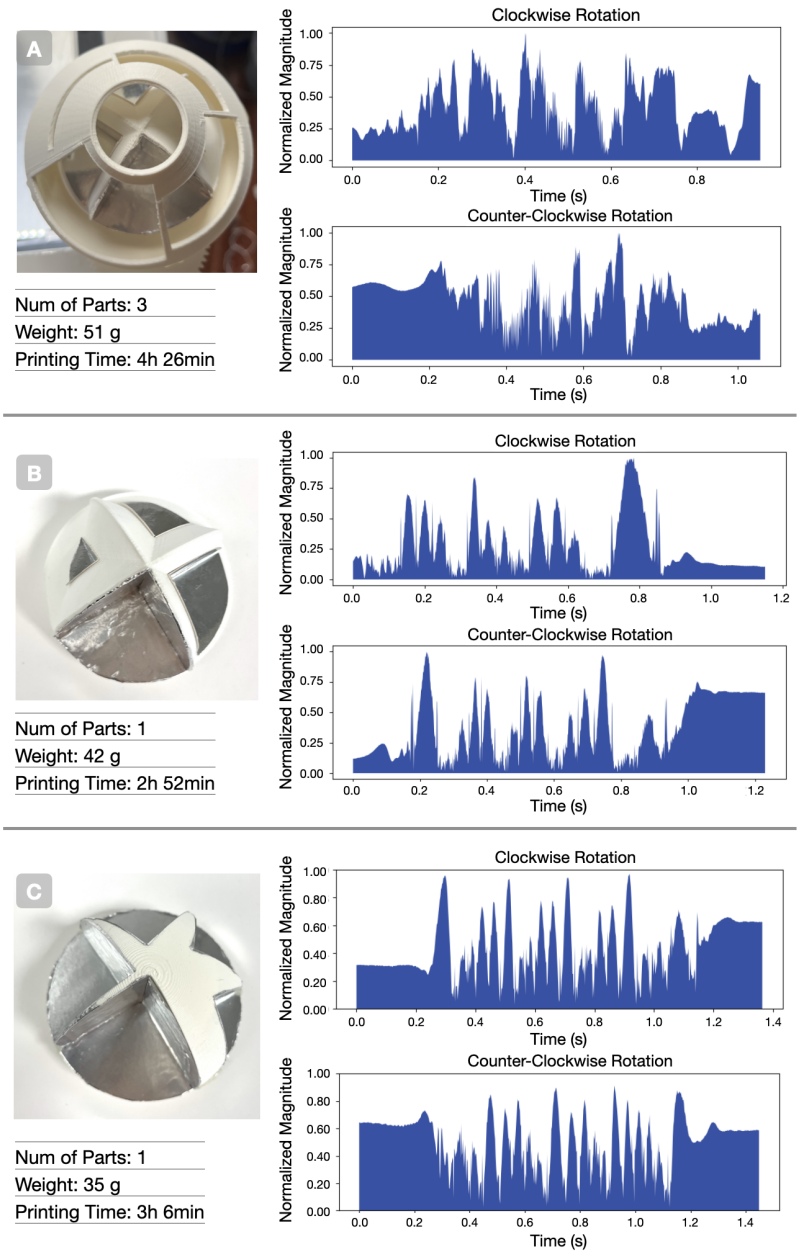

Figure 4.5: Geometry and signals of different reflectors. The weight and printing time are approximated based on the printing parameters used with the Ultimaker S5 3D Printer [S523], including a layer height of 0.2 mm and 10 % infill. A: Reflector with cone-shaped shield. B: Hemisphere-shaped reflector with four parallel pockets. C: Hemisphere-shaped reflector with computationally designed pockets.

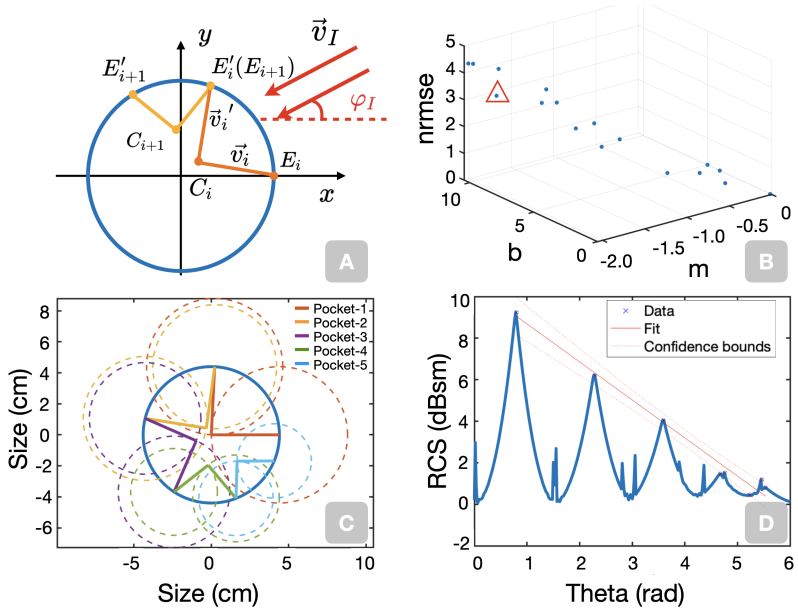

Figure 4.6: A: Top view of the hemisphere-shaped reflector, pocket arrangement and incident waves. B: Objective values of 18 solutions. C: Top view of reflector with radius=4.4, 4.0, 3.6, 2.8, 2.6 cm for pocket 1 - 5. D: Simulated RCS (i.e., H) of the reflector, peaks and the fitted model.

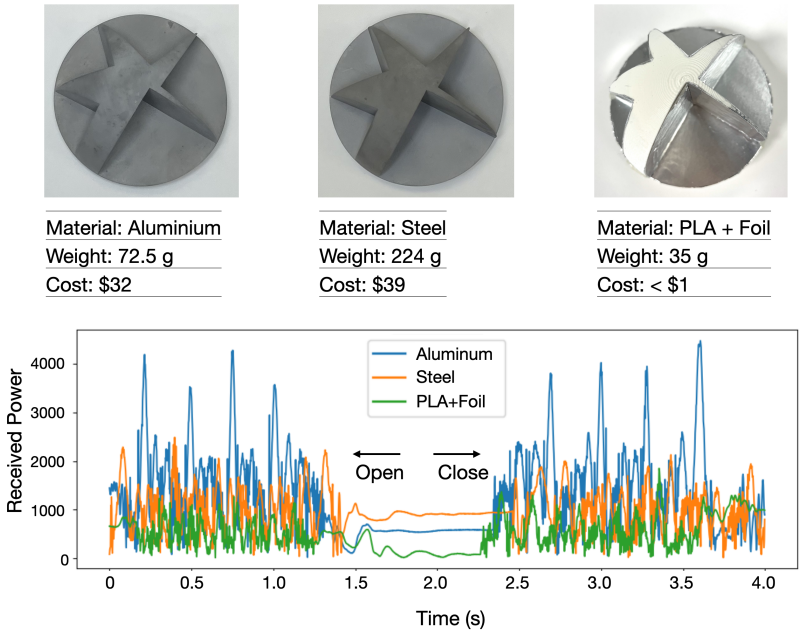

Figure 4.7: Reflectors made of Aluminium, Steel, and PLA; their fabrication details; and their signals collected from a mmWave radar positioned at 2.6 m away.

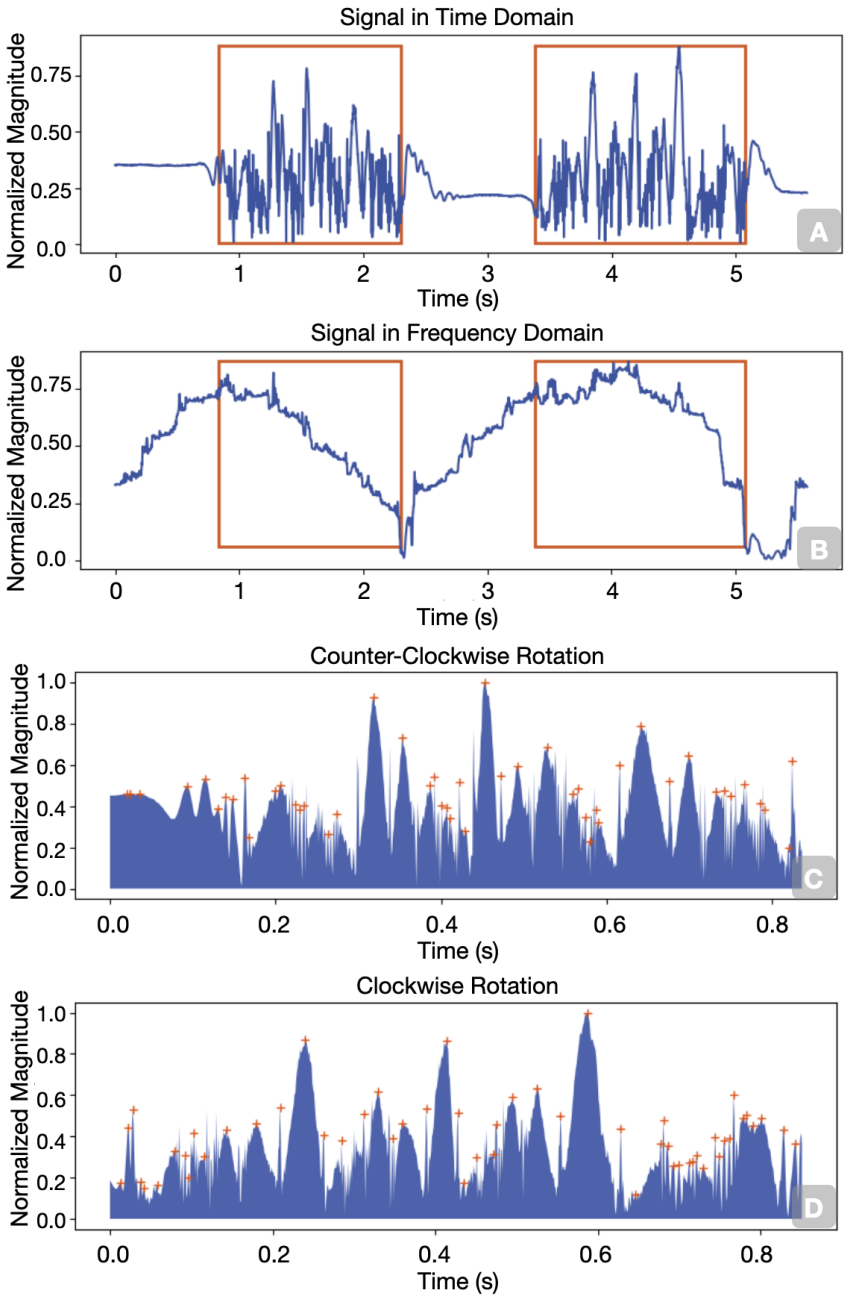

Figure 4.8: A: Signals of a single trial of opening and closing the CNC enclosure. B is obtained by applying FFT to signals within a window (size=512) that slides along the time axis and sums the high frequency components (larger than 50 Hz). C and D are signals from the two specific regions of A, with orange crosshairs representing the detected peaks.

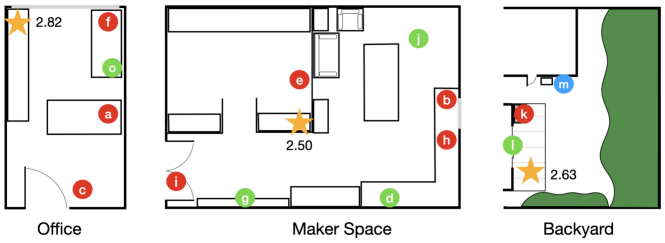

Location	Object	Distance to sensor (m)	Event Existence Detection		Direction Detection	
			Quiet Environment	Occupied Environment	Quiet Environment	Occupied Environment
Office	Table Lamp (f)	2.52	0.90	0.97	0.72	0.72
	Microwave (a)	3.02	1.00	1.00	0.83	0.78
	Trash Bin (c)	3.97	0.98	0.98	0.83	0.80
	Standing Desk (o)	2.85	0.97	0.97	0.80	0.82
Maker Space	CNC Machine (b)	3.22	0.98	0.98	0.82	0.83
	Backdrop (d)	3.07	0.93	0.97	0.70	0.75
	Fridge (e)	2.72	0.98	0.93	0.75	0.80
	Storage Container (g)	3.00	1.00	1.00	0.87	0.83
	3D Printer (h)	4.65	1.00	1.00	0.80	0.75
	Hinged Door (i)	5.20	0.98	0.97	0.68	0.72
	Treadmill (j)	3.80	1.00	1.00	–	
Backyard	Grill (k)	2.50	1.00	1.00	0.82	0.85
	Sliding Door (l)	1.94	1.00	1.00	0.82	0.85
	Faucet (m)	5.52	0.97	0.97	–	

Figure 4.9: Deployment details. Left: Floor plans of the three locations in the evaluation. Colored dots are objects instrumented with mechanisms as shown in Figure 4.4. The orange stars denote the radar sensor with the number indicating its height to the ground (in meters). Right: Detection accuracies. Note that the treadmill and faucet are unidirectional objects and were excluded from the evaluation of the direction detection.

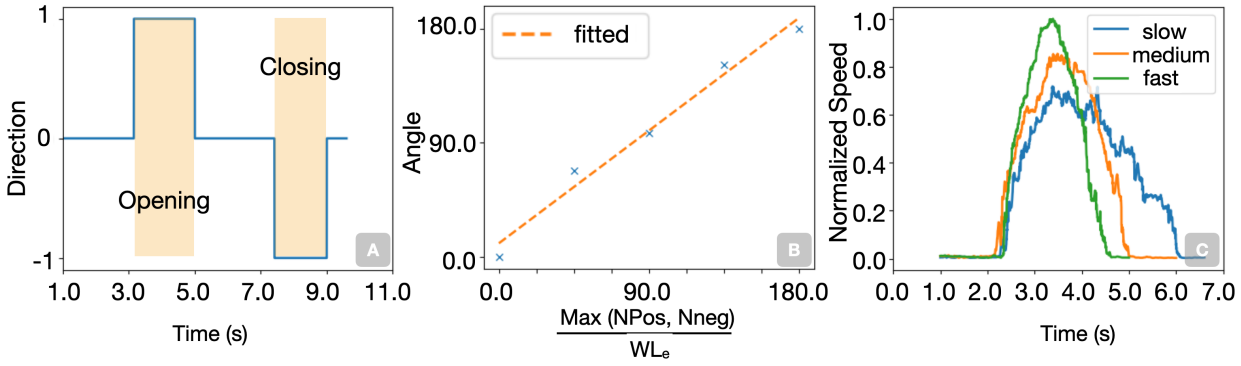

Figure 4.10: Fine-grained information about activities including direction (A), angle (B), and speed (C) can be detected.

Algorithm 1 Event detection algorithm

Input: signal sequence $w_1, w_2, ..., w_n$
Output: $Presence, Speed, Angle, Direction$

while w_i received **do**
  $f_{w_i} = FFT(w_i)$, apply a low pass filter on f_{w_i}
  sum high frequency bins of f_{w_i} to obtain f_{hf}
  if $f_{hf} \in (Thred_{high}, Thred_{low})$ **then**
    presence = true -> **presence**
  end if
  $peaks = findPeaks(w_i, PW)$
  calculate derivative of $peaks$, count number of positive derivative $NPos$ and negative derivative $NNeg$
end while
obtain w_e from all w_i with $Presence = true$
while w_e exists, window size WL_e **do**
  $peaks_e = findPeaks(w_e, PW)$
  calculate derivative $peaks_{diff}$
  get $idx = max(abs(peaks_{diff}))$
  direction $\propto$ polarity of $peaks_{diff}(idx)$ -> **direction**
  angle $\propto \frac{\max(NPos,NNeg)}{WL_e}$ -> **angle**
  speed $\propto f_{hf}$ -> **speed**
end while

Figure 4.11: Event detection algorithm.

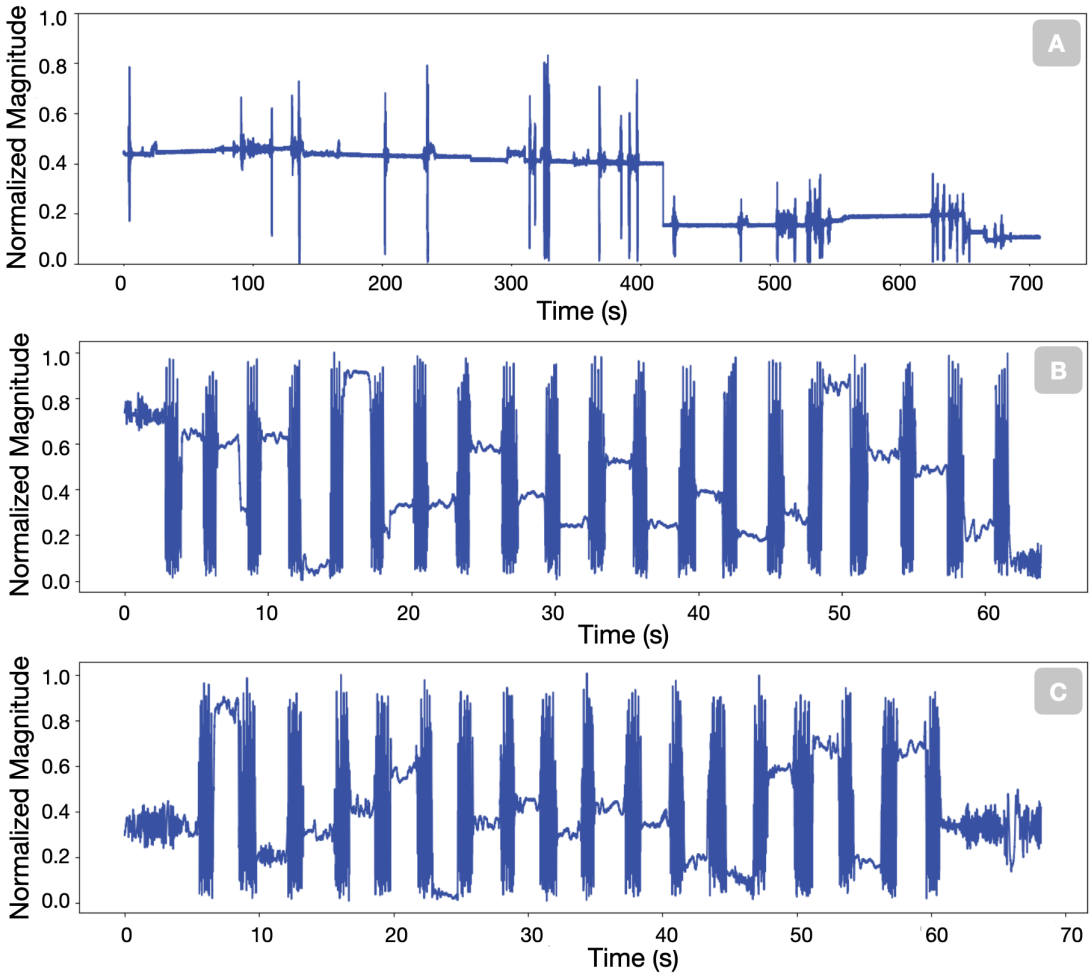

Figure 4.12: A round of testing for the storage container. Ten minutes of data collected when no objects were in use in an occupied environment (A). One minute of 10 trials of operation in a quiet environment (B) and in a busy environment where people were walking around (C).

CHAPTER 5

Conclusion

The main goal of this thesis is to explore how interaction power can be utilized as an energy source to extend the longevity of IoT applications and eliminate the necessity for frequent battery maintenance. More specifically, this thesis demonstrated preliminary explorations into employing interaction power for executing actuation and sensing tasks of IoT.

In Chapter 2, we conducted benchmark tests to understand the characteristics of interaction power, from which we established the correlation between the amount of energy harvested, the configurations of motor harvesters and the patterns of user motions. With these findings, we presented MiniKers in Chapter 3, an fleet of interaction-powered environment automation devices. We demonstrated a comprehensive design scheme of MiniKers, including mechanical designs, circuits and phone apps. We conducted a series of technical validations and a 48-hour deployment study of 9 objects to prove the efficacy of our system. In Chapter 4, we introduced a new method of transforming interaction power to RF backscatter to mmWave radar for detecting activities in user environments. We proposed a computational approach to design reflector mechanisms and conducted studies on 15 objects at three different locations, which demonstrated the robustness of our approach with extremely low false positive rates.

Our work in this thesis has shown the feasibility of using interaction power for IoT actuation and sensing. We envision our approach to be integrated into future IoT devices such as automatic doors, curtains, smart light bulbs, speakers, and service robots, to extend their lifespan, enhance their capacity to infer user context and thus improve their capability

to serve.

There are multiple future research opportunities on interaction-powered IoT. A systematic study can be conducted to quantify the amount of interaction energy from various body movements, including actions like pushing, cranking, and stepping, providing foundational benchmarks for designing harvesters. The usability of interaction-powered IoT devices should be properly investigated in future work, including frequency of interactions in different environments and applications and user perceptions to harvesters. In addition, interaction power, characterized by its unique property of existing only during interactions, holds promise for improving security and privacy in IoT applications. We also seek to extend interaction power to a wider range of computing by delivering interaction power to other device modalities and thus extending the applications of interaction harvesting.

All in all, this thesis creatively proposed the utilization of people interactions as the energy sources to power IoT applications, which has the potential to advance the large scale deployment of IoT technologies.

REFERENCES

[AA18] Nivedita Arora and Gregory D Abowd. "ZEUSSS: Zero energy ubiquitous sound sensing surface leveraging triboelectric nanogenerator and analog backscatter communication." In *The 31st Annual ACM Symposium on User Interface Software and Technology Adjunct Proceedings*, pp. 81–83, 2018.

[ADT17] VS Asadchy, Ana Díaz-Rubio, SN Tcvetkova, D-H Kwon, Amr Elsakka, Mohamed Albooyeh, and SA Tretyakov. "Flat engineered multichannel reflectors." *Physical Review X*, **7**(3):031046, 2017.

[ALC22] Abul Al Arabi, Jiahao Li, Xiang'Anthony Chen, and Jeeeun Kim. "Mobiot: Augmenting Everyday Objects into Moving IoT Devices Using 3D Printed Attachments Generated by Demonstration." In *CHI Conference on Human Factors in Computing Systems*, pp. 1–14, 2022.

[AMM21] Nivedita Arora, Ali Mirzazadeh, Injoo Moon, Charles Ramey, Yuhui Zhao, Daniela C Rodriguez, Gregory D Abowd, and Thad Starner. "MARS: Nano-Power Battery-free Wireless Interfaces for Touch, Swipe and Speech Input." In *The 34th Annual ACM Symposium on User Interface Software and Technology*, pp. 1305–1325, 2021.

[Aut22] ZED Automation. "Automatic Door.", 2022. Last accessed 12 May 2022.

[AYT21] Rebecca Adaimi, Howard Yong, and Edison Thomaz. "Ok Google, What Am I Doing? Acoustic Activity Recognition Bounded by Conversational Assistant Interactions." *Proc. ACM Interact. Mob. Wearable Ubiquitous Technol.*, **5**(1), mar 2021.

[AZS18] Nivedita Arora, Steven L Zhang, Fereshteh Shahmiri, Diego Osorio, Yi-Cheng Wang, Mohit Gupta, Zhengjun Wang, Thad Starner, Zhong Lin Wang, and Gregory D Abowd. "SATURN: A thin and flexible self-powered microphone leveraging triboelectric nanogenerator." *Proceedings of the ACM on Interactive, Mobile, Wearable and Ubiquitous Technologies*, **2**(2):1–28, 2018.

[BCD08] Aude Billard, Sylvain Calinon, Ruediger Dillmann, and Stefan Schaal. "Robot programming by demonstration." *Springer handbook of robotics*, pp. 1371–1394, 2008.

[BOC18] Mayara Bonani, Raquel Oliveira, Filipa Correia, André Rodrigues, Tiago Guerreiro, and Ana Paiva. "What my eyes can't see, A robot can show me: Exploring the collaboration between blind people and robots." In *Proceedings of the 20th International ACM SIGACCESS Conference on Computers and Accessibility*, pp. 15–27, 2018.

[BPB19] Christian Buchberger, Florian Pfeiffer, and Erwin Biebl. "Dielectric corner reflectors for mmWave applications." *Advances in Radio Science*, **17**:197–203, 2019.

[BPP09a] Michael Buettner, Richa Prasad, Matthai Philipose, and David Wetherall. "Recognizing Daily Activities with RFID-Based Sensors." In *Proceedings of the 11th International Conference on Ubiquitous Computing*, UbiComp '09, p. 51–60, New York, NY, USA, 2009. Association for Computing Machinery.

[BPP09b] Michael Buettner, Richa Prasad, Matthai Philipose, and David Wetherall. "Recognizing Daily Activities with RFID-Based Sensors." In *Proceedings of the 11th International Conference on Ubiquitous Computing*, UbiComp '09, p. 51–60, New York, NY, USA, 2009. Association for Computing Machinery.

[CD14] Bradford Campbell and Prabal Dutta. "An energy-harvesting sensor architecture and toolkit for building monitoring and event detection." In *Proceedings of the 1st ACM Conference on Embedded Systems for Energy-Efficient Buildings*, pp. 100–109, 2014.

[Cen77] Yair Censor. "Pareto optimality in multiobjective problems." *Applied Mathematics and Optimization*, **4**(1):41–59, 1977.

[CGL12] Gabe Cohn, Sidhant Gupta, Tien-Jui Lee, Dan Morris, Joshua R Smith, Matthew S Reynolds, Desney S Tan, and Shwetak N Patel. "An ultra-low-power human body motion sensor using static electric field sensing." In *Proceedings of the 2012 ACM conference on ubiquitous computing*, pp. 99–102, 2012.

[CGL15] Ke-Yu Chen, Sidhant Gupta, Eric C. Larson, and Shwetak Patel. "DOSE: Detecting user-driven operating states of electronic devices from a single sensing point." In *2015 IEEE International Conference on Pervasive Computing and Communications (PerCom)*, pp. 46–54, 2015.

[CKL21] Hyungjun Cho, Han-Jong Kim, JiYeon Lee, Chang-Min Kim, Jinseong Bae, and Tek-Jin Nam. "IoTIZER: A Versatile Mechanical Hijacking Device for Creating Internet of Old Things." In *Designing Interactive Systems Conference 2021*, pp. 90–103, 2021.

[CLC10] Tim Campbell, Eric Larson, Gabe Cohn, Jon Froehlich, Ramses Alcaide, and Shwetak N Patel. "WATTR: A method for self-powered wireless sensing of water activity in the home." In *Proceedings of the 12th ACM international conference on Ubiquitous computing*, pp. 169–172, 2010.

[CLL20] Baicheng Chen, Huining Li, Zhengxiong Li, Xingyu Chen, Chenhan Xu, and Wenyao Xu. "ThermoWave: a new paradigm of wireless passive temperature monitoring via mmWave sensing." In *Proceedings of the 26th Annual International Conference on Mobile Computing and Networking*, pp. 1–14, 2020.

[clo22] Automatic door closer, 2022. Last accessed 20 July 2022.

[CR16] Peter Constantinou and Saibal Roy. "A 3D printed electromagnetic nonlinear vibration energy harvester." *Smart Materials and Structures*, **25**(9):095053, 2016.

[CRB21] Alexander Curtiss, Blaine Rothrock, Abu Bakar, Nivedita Arora, Jason Huang, Zachary Englhardt, Aaron-Patrick Empedrado, Chixiang Wang, Saad Ahmed, Yang Zhang, et al. "FaceBit: Smart Face Masks Platform." *Proceedings of the ACM on Interactive, Mobile, Wearable and Ubiquitous Technologies*, **5**(4):1–44, 2021.

[CST23] Software Information. CST. CST n.d.. CST STUDIO SUITE, 2023. Last accessed 20 March 2023.

[Dat22] World Energy Data. "World Final Energy.", 2022. Last accessed 23 July 2022.

[DB09] Armin W Doerry and Billy C Brock. "Radar cross section of triangular trihedral reflector with extended bottom plate." *Sandia Report, Sandia National Laboratory*, 2009.

[DCD13] Samuel DeBruin, Bradford Campbell, and Prabal Dutta. "Monjolo: An energy-harvesting energy meter architecture." In *Proceedings of the 11th ACM Conference on Embedded Networked Sensor Systems*, pp. 1–14, 2013.

[DHW18] Qinglang Dai, Yongzhi Huang, Lu Wang, Rukhsana Ruby, and Kaishun Wu. "mm-humidity: Fine-grained humidity sensing with millimeter wave signals." In *2018 IEEE 24th International Conference on Parallel and Distributed Systems (ICPADS)*, pp. 204–211. IEEE, 2018.

[DKH20] Jasper De Winkel, Vito Kortbeek, Josiah Hester, and Przemysław Pawełczak. "Battery-free game boy." *Proceedings of the ACM on Interactive, Mobile, Wearable and Ubiquitous Technologies*, **4**(3):1–34, 2020.

[Doe14] Armin Walter Doerry. "Reflectors for SAR performance testing." Technical report, Sandia National Lab.(SNL-NM), Albuquerque, NM (United States), 2014.

[DVT11] Scott Davidoff, Nicolas Villar, Alex S Taylor, and Shahram Izadi. "Mechanical hijacking: how robots can accelerate UbiComp deployments." In *Proceedings of the 13th international conference on Ubiquitous computing*, pp. 267–270. ACM, 2011.

[Eck71] HD Eckhardt. "Simple model of corner reflector phenomena." *Applied Optics*, **10**(7):1559–1566, 1971.

[equ23] Fresnel equation, 2023. Last accessed 20 March 2023.

[ERZ01] Markus Ehrenmann, Oliver Rogalla, Raoul Zöllner, and Rüdiger Dillmann. "Teaching service robots complex tasks: Programming by demonstration for workshop and household environments." In *Proceedings of the 2001 International Conference on Field and Service Robots (FSR)*, volume 1, pp. 397–402, 2001.

[FAL19] Nathaniel Faulkner, Fakhrul Alam, Mathew Legg, and Serge Demidenko. "Watchers on the wall: Passive visible light-based positioning and tracking with embedded light-sensors on the wall." *IEEE Transactions on Instrumentation and Measurement*, **69**(5):2522–2532, 2019.

[FEP16] David Fischinger, Peter Einramhof, Konstantinos Papoutsakis, Walter Wohlkinger, Peter Mayer, Paul Panek, Stefan Hofmann, Tobias Koertner, Astrid Weiss, Antonis Argyros, et al. "Hobbit, a care robot supporting independent living at home: First prototype and lessons learned." *Robotics and Autonomous Systems*, **75**:60–78, 2016.

[FLZ21] Chao Feng, Xinyi Li, Yangfan Zhang, Xiaojing Wang, Liqiong Chang, Fuwei Wang, Xinyu Zhang, and Xiaojiang Chen. "RFlens: metasurface-enabled beamforming for IoT communication and sensing." In *Proceedings of the 27th Annual International Conference on Mobile Computing and Networking*, pp. 587–600, 2021.

[GHC16] Tobias Grosse-Puppendahl, Steve Hodges, Nicholas Chen, John Helmes, Stuart Taylor, James Scott, Josh Fromm, and David Sweeney. "Exploring the design space for energy-harvesting situated displays." In *Proceedings of the 29th Annual Symposium on User Interface Software and Technology*, pp. 41–48, 2016.

[GHP22] Tamil Selvan Gunasekaran, Ryo Hajika, Yun Suen Pai, Eiji Hayashi, and Mark Billinghurst. "RaITIn: Radar-Based Identification for Tangible Interactions." CHI EA '22, New York, NY, USA, 2022. Association for Computing Machinery.

[GPW18] Manoj Gulati, Farshid Salemi Parizi, Eric Whitmire, Sidhant Gupta, Shobha Sundar Ram, Amarjeet Singh, and Shwetak N. Patel. "CapHarvester: A Stick-on Capacitive Energy Harvester Using Stray Electric Field from AC Power Lines." *Proc. ACM Interact. Mob. Wearable Ubiquitous Technol.*, **2**(3):110:1–110:20, September 2018.

[GRP10] Sidhant Gupta, Matthew S. Reynolds, and Shwetak N. Patel. "ElectriSense: Single-Point Sensing Using EMI for Electrical Event Detection and Classification in the Home." In *Proceedings of the 12th ACM International Conference on Ubiquitous Computing*, UbiComp '10, p. 139–148, New York, NY, USA, 2010. Association for Computing Machinery.

[GVL90] A Laurence Gray, Paris W Vachon, Charles E Livingstone, and Tom I Lukowski. "Synthetic aperture radar calibration using reference reflectors." *IEEE Transactions on Geoscience and Remote Sensing*, **28**(3):374–383, 1990.

[HJ14] Guy Hoffman and Wendy Ju. "Designing Robots With Movement in Mind." *Journal of Human-Robot Interaction*, 2014.

[HLG21] Eiji Hayashi, Jaime Lien, Nicholas Gillian, Leonardo Giusti, Dave Weber, Jin Yamanaka, Lauren Bedal, and Ivan Poupyrev. "RadarNet: Efficient Gesture Recognition Technique Utilizing a Miniature Radar Sensor." In *Proceedings of the 2021 CHI Conference on Human Factors in Computing Systems*, CHI '21, New York, NY, USA, 2021. Association for Computing Machinery.

[HOM22] HC SMART HOME. "HC SMART HOME.", 2022. Last accessed 12 May 2022.

[HS17] Josiah Hester and Jacob Sorber. "The future of sensing is batteryless, intermittent, and awesome." In *Proceedings of the 15th ACM conference on embedded network sensor systems*, pp. 1–6, 2017.

[HTY21] Jianghaomiao He, Shota Terashima, Hideyuki Yamada, and Shouhei Kidera. "Diffraction signal-based human recognition in non-line-of-sight (NLOS) situation for millimeter wave radar." *IEEE Journal of Selected Topics in Applied Earth Observations and Remote Sensing*, **14**:4370–4380, 2021.

[HWW21] Yuqian Hu, Beibei Wang, Chenshu Wu, and KJ Ray Liu. "mmKey: Universal Virtual Keyboard Using A Single Millimeter-Wave Radio." *IEEE Internet of Things Journal*, **9**(1):510–524, 2021.

[ICG17] Vikram Iyer, Justin Chan, and Shyamnath Gollakota. "3D Printing Wireless Connected Objects." ACM, 2017.

[INR16] Mohamed Ibrahim, Viet Nguyen, Siddharth Rupavatharam, Minitha Jawahar, Marco Gruteser, and Richard Howard. "Visible Light Based Activity Sensing Using Ceiling Photosensors." In *Proceedings of the 3rd Workshop on Visible Light Communication Systems*, VLCS '16, p. 43–48, New York, NY, USA, 2016. Association for Computing Machinery.

[Int22] Solar Lighting International. "LED Solar Powered Street Lighting.", 2022. Last accessed 14 May 2022.

[JGe17] JGendron. "RobotShop Announces Canada and Europe Distribution Exclusivity with Solar Pool Technologies.", 2017. Last accessed 24 April 2022.

[JGH20] Chengkun Jiang, Junchen Guo, Yuan He, Meng Jin, Shuai Li, and Yunhao Liu. "mmVib: micrometer-level vibration measurement with mmwave radar." In *Proceedings of the 26th Annual International Conference on Mobile Computing and Networking*, pp. 1–13, 2020.

[JSE20] Alejandro Jiménez-Sáez, Martin Schüßler, Mohammed El-Absi, Ali Alhaj Abbas, Klaus Solbach, Thomas Kaiser, and Rolf Jakoby. "Frequency selective surface coded retroreflectors for chipless indoor localization tag landmarks." *IEEE Antennas and Wireless Propagation Letters*, **19**(5):726–730, 2020.

[JWY18] Haojian Jin, Jingxian Wang, Zhijian Yang, Swarun Kumar, and Jason Hong. "Wish: Towards a wireless shape-aware world using passive rfids." In *Proceedings of the 16th Annual International Conference on Mobile Systems, Applications, and Services*, pp. 428–441, 2018.

[Kas22] Kasa. "Smart Wi-Fi Light Switch, Dimmer.", 2022.

[Key22] KeyiRobot. "Coding Fun Robot for Steam Learning.", 2022. Last accessed 12 May 2022.

[KFA19] Daniel Konings, Nathaniel Faulkner, Fakhrul Alam, Edmund M-K Lai, and Serge Demidenko. "FieldLight: Device-free indoor human localization using passive visible light positioning and artificial potential fields." *IEEE Sensors Journal*, **20**(2):1054–1066, 2019.

[KGP18] Ioannis Kostavelis, Dimitrios Giakoumis, Georgia Peleka, Andreas Kargakos, Evangelos Skartados, Manolis Vasileiadis, and Dimitrios Tzovaras. "RAMCIP robot: A personal robotic assistant; demonstration of a complete framework." In *Proceedings of the European conference on computer vision (ECCV) workshops*, pp. 0–0, 2018.

[KHT21] Haruka Kamachi, Tahera Hossain, Fuyuka Tokuyama, Anna Yokokubo, and Guillaume Lopez. "Prediction of Eating Activity Using Smartwatch." In *Adjunct Proceedings of the 2021 ACM International Joint Conference on Pervasive and Ubiquitous Computing and Proceedings of the 2021 ACM International Symposium on Wearable Computers*, UbiComp '21, p. 304–309, New York, NY, USA, 2021. Association for Computing Machinery.

[KP10] Stacey Kuznetsov and Eric Paulos. "UpStream: motivating water conservation with low-cost water flow sensing and persuasive displays." In *Proceedings of the SIGCHI Conference on Human Factors in Computing Systems*, pp. 1851–1860, 2010.

[KPF13] Mustafa Emre Karagozler, Ivan Poupyrev, Gary K Fedder, and Yuri Suzuki. "Paper generators: harvesting energy from touching, rubbing and sliding." In *Proceedings of the 26th annual ACM symposium on User interface software and technology*, pp. 23–30, 2013.

[KSL20] Bartosz Kawa, Krzysztof Śliwa, Vincent Ch Lee, Qiongfeng Shi, and Rafał Walczak. "Inkjet 3D printed MEMS vibrational electromagnetic energy harvester." *Energies*, **13**(11):2800, 2020.

[KXY22] Hao Kong, Xiangyu Xu, Jiadi Yu, Qilin Chen, Chenguang Ma, Yingying Chen, Yi-Chao Chen, and Linghe Kong. "m3track: mmwave-based multi-user 3d posture tracking." In *Proceedings of the 20th Annual International Conference on Mobile Systems, Applications and Services*, pp. 491–503, 2022.

[KYT19] Tarik Keleştemur, Naoki Yokoyama, Joanne Truong, Anas Abou Allaban, and Taşkin Padir. "System architecture for autonomous mobile manipulation of everyday objects in domestic environments." In *Proceedings of the 12th ACM International Conference on PErvasive Technologies Related to Assistive Environments*, pp. 264–269, 2019.

[lab22] Ecube labs. "CleanCUBE, the solar-powered trash compactor.", 2022. Last accessed 14 May 2022.

[LCK20] Jiahao Li, Meilin Cui, Jeeeun Kim, and Xiang'Anthony' Chen. "Romeo: A Design Tool for Embedding Transformable Parts in 3D Models to Robotically Augment Default Functionalities." In *Proceedings of the 33rd Annual ACM Symposium on User Interface Software and Technology*, pp. 897–911, 2020.

[LCY19] Zhengxiong Li, Baicheng Chen, Zhuolin Yang, Huining Li, Chenhan Xu, Xingyu Chen, Kun Wang, and Wenyao Xu. "Ferrotag: A paper-based mmwave-scannable tagging infrastructure." In *Proceedings of the 17th Conference on Embedded Networked Sensor Systems*, pp. 324–337, 2019.

[LGK16] Jaime Lien, Nicholas Gillian, M. Emre Karagozler, Patrick Amihood, Carsten Schwesig, Erik Olson, Hakim Raja, and Ivan Poupyrev. "Soli: Ubiquitous Gesture Sensing with Millimeter Wave Radar." *ACM Trans. Graph.*, **35**(4), jul 2016.

[LH19] Gierad Laput and Chris Harrison. "Sensing Fine-Grained Hand Activity with Smartwatches." In *Proceedings of the 2019 CHI Conference on Human Factors in Computing Systems*, CHI '19, p. 1–13, New York, NY, USA, 2019. Association for Computing Machinery.

[Lin14] Zhong Lin Wang. "Triboelectric nanogenerators as new energy technology and self-powered sensors–Principles, problems and perspectives." *Faraday discussions*, **176**:447–458, 2014.

[LKC19] Jiahao Li, Jeeeun Kim, and Xiang'Anthony' Chen. "Robiot: A design tool for actuating everyday objects with automatically generated 3D printable mechanisms." In *Proceedings of the 32nd Annual ACM Symposium on User Interface Software and Technology*, pp. 673–685, 2019.

[LLL18] Shengjie Li, Xiang Li, Qin Lv, Guiyu Tian, and Daqing Zhang. "WiFit: Ubiquitous bodyweight exercise monitoring with commodity wi-fi devices." In *2018 IEEE SmartWorld, Ubiquitous Intelligence & Computing, Advanced*

& Trusted Computing, Scalable Computing & Communications, Cloud & Big Data Computing, Internet of People and Smart City Innovation (SmartWorld/SCALCOM/UIC/ATC/CBDCom/IOP/SCI), pp. 530–537. IEEE, 2018.

[LLP18] Yichen Li, Tianxing Li, Ruchir A Patel, Xing-Dong Yang, and Xia Zhou. "Self-powered gesture recognition with ambient light." In *Proceedings of the 31st Annual ACM Symposium on User Interface Software and Technology*, pp. 595–608, 2018.

[Log21] LogiTech. "K750 Wireless Solar Powered Keyboard.", 2021. Last accessed 24 April 2022.

[LSK22] Jiahao Li, Alexis Samoylov, Jeeeun Kim, and Xiang'Anthony' Chen. "Roman: Making Everyday Objects Robotically Manipulable with 3D-Printable Add-on Mechanisms." In *CHI Conference on Human Factors in Computing Systems*, pp. 1–17, 2022.

[LXH16] Gierad Laput, Robert Xiao, and Chris Harrison. "ViBand: High-Fidelity Bio-Acoustic Sensing Using Commodity Smartwatch Accelerometers." In *Proceedings of the 29th Annual Symposium on User Interface Software and Technology*, UIST '16, p. 321–333, New York, NY, USA, 2016. Association for Computing Machinery.

[LYS15] Hanchuan Li, Can Ye, and Alanson P. Sample. "IDSense: A Human Object Interaction Detection System Based on Passive UHF RFID." In *Proceedings of the 33rd Annual ACM Conference on Human Factors in Computing Systems*, CHI '15, p. 2555–2564, New York, NY, USA, 2015. Association for Computing Machinery.

[Mat22] Cable Matters. "Self Powered Wireless Doorbell Kit.", 2022.

[MGD22] Francesca Meneghello, Domenico Garlisi, Nicolò Dal Fabbro, Ilenia Tinnirello, and Michele Rossi. "SHARP: Environment and Person Independent Activity Recognition with Commodity IEEE 802.11 Access Points." *IEEE Transactions on Mobile Computing*, 2022.

[MGL10] Andrew Meehan, Hongwei Gao, and Zbigniew Lewandowski. "Energy harvesting with microbial fuel cell and power management system." *IEEE Transactions on power electronics*, **26**(1):176–181, 2010.

[Mic22] Microbot. "MicroBot Push.", 2022. Last accessed 12 May 2022.

[Mob22] 101 Mobility. "Automatic Door Openers.", 2022. Last accessed 12 May 2022.

[MP22] Gabriel Marcano and Pat Pannuto. "Soil Power? Can Microbial Fuel Cells Power Non-Trivial Sensors." In *Proceedings of the 1st ACM Workshop on No Power and Low Power Internet-of-Things (New Orleans, LA, USA)(LP-IoT'21)*, pp. 8–13, 2022.

[Nor22] Nordic. "nRF52832 Product Specification.", 2022. Last accessed 12 May 2022.

[NQZ21] John Nolan, Kun Qian, and Xinyu Zhang. "RoS: passive smart surface for roadside-to-vehicle communication." In *Proceedings of the 2021 ACM SIGCOMM 2021 Conference*, pp. 165–178, 2021.

[OWW21] Muhammed Zahid Ozturk, Chenshu Wu, Beibei Wang, and KJ Liu. "Radiomic: Sound sensing via mmwave signals." *arXiv preprint arXiv:2108.03164*, 2021.

[per23] Relative permittivity, 2023. Last accessed 27 July 2023.

[Phi22] Philips. "Light hub.", 2022. Last accessed 20 July 2022.

[PRA08] Shwetak N Patel, Matthew S Reynolds, and Gregory D Abowd. "Detecting human movement by differential air pressure sensing in HVAC system ductwork: An exploration in infrastructure mediated sensing." In *Pervasive Computing: 6th International Conference, Pervasive 2008 Sydney, Australia, May 19-22, 2008 Proceedings 6*, pp. 1–18. Springer, 2008.

[PRC19] Samuel Poirier, François Routhier, and Alexandre Campeau-Lecours. "Voice control interface prototype for assistive robots for people living with upper limb disabilities." In *2019 IEEE 16th International Conference on Rehabilitation Robotics (ICORR)*, pp. 46–52. IEEE, 2019.

[PS13] Michaël Peigney and Dominique Siegert. "Piezoelectric energy harvesting from traffic-induced bridge vibrations." *Smart Materials and Structures*, **22**(9):095019, 2013.

[PSO16] Kyle Pietrzyk, Joseph Soares, Brandon Ohara, and Hohyun Lee. "Power generation modeling for a wearable thermoelectric energy harvester with practical limitations." *Applied energy*, **183**:218–228, 2016.

[Q22] My Q. "Smart Locks.", 2022. Last accessed 12 May 2022.

[qua23] Radar quation, 2023. Last accessed 20 March 2023.

[QYZ22] Kun Qian, Lulu Yao, Xinyu Zhang, and Tse Nga Ng. "MilliMirror: 3D Printed Reflecting Surface for Millimeter-Wave Coverage Expansion." MobiCom '22, p. 15–28, New York, NY, USA, 2022. Association for Computing Machinery.

[RAG16] Raf Ramakers, Fraser Anderson, Tovi Grossman, and George Fitzmaurice. "Retrofab: A design tool for retrofitting physical interfaces using actuators, sensors and 3d printing." In *Proceedings of the 2016 CHI Conference on Human Factors in Computing Systems*, pp. 409–419, 2016.

[ref23] Corner reflector, 2023. Last accessed 24 July 2023.

[rin23] Oura smart ring, 2023. Last accessed 20 March 2023.

[RPS22] Michaela R Reisinger, Sebastian Prost, Johann Schrammel, and Peter Fröhlich. "User requirements for the design of smart homes: dimensions and goals." *Journal of Ambient Intelligence and Humanized Computing*, pp. 1–20, 2022.

[RSK14] Kimiko Ryokai, Peiqi Su, Eungchan Kim, and Bob Rollins. "Energybugs: Energy harvesting wearables for children." In *Proceedings of the SIGCHI Conference on Human Factors in Computing Systems*, pp. 1039–1048, 2014.

[S523] Ultimaker S5, 2023. Last accessed 20 July 2023.

[SCZ20] Wei Sun, Tuochao Chen, Jiayi Zheng, Zhenyu Lei, Lucy Wang, Benjamin Steeper, Peng He, Matthew Dressa, Feng Tian, and Cheng Zhang. "VibroSense: Recognizing Home Activities by Deep Learning Subtle Vibrations on an Interior Surface of a House from a Single Point Using Laser Doppler Vibrometry." *Proc. ACM Interact. Mob. Wearable Ubiquitous Technol.*, **4**(3), sep 2020.

[See22] Johny's Selected Seeds. "Green House Auto Ven Opener.", 2022. Last accessed 12 May 2022.

[Sen22] Senic. "Battery free and wireless switches.", 2022.

[SHK17] Farhad Shahmohammadi, Anahita Hosseini, Christine E King, and Majid Sarrafzadeh. "Smartwatch based activity recognition using active learning." In *2017 IEEE/ACM International Conference on Connected Health: Applications, Systems and Engineering Technologies (CHASE)*, pp. 321–329. IEEE, 2017.

[SKT16] Pavle Skocir, Petar Krivic, Matea Tomeljak, Mario Kusek, and Gordan Jezic. "Activity detection in smart home environment." *Procedia Computer Science*, **96**:672–681, 2016.

[sol22] Smart home solutions, 2022. Last accessed 20 July 2022.

[Som22] Somfy. "Somfy: Motorization solutions for a smarter home inside out.", 2022. Last accessed 12 May 2022.

[SP04] Thad Starner and Joseph A Paradiso. "Human generated power for mobile electronics." *Low-power electronics design*, **45**:1–35, 2004.

[SPB21] Elahe Soltanaghaei, Akarsh Prabhakara, Artur Balanuta, Matthew Anderson, Jan M. Rabaey, Swarun Kumar, and Anthony Rowe. "Millimetro: MmWave Retro-Reflective Tags for Accurate, Long Range Localization." In *Proceedings of the 27th Annual International Conference on Mobile Computing and Networking*, MobiCom '21, p. 69–82, New York, NY, USA, 2021. Association for Computing Machinery.

[SSG19] Akash Deep Singh, Sandeep Singh Sandha, Luis Garcia, and Mani Srivastava. "RadHAR: Human Activity Recognition from Point Clouds Generated through a Millimeter-Wave Radar." In *Proceedings of the 3rd ACM Workshop on Millimeter-Wave Networks and Sensing Systems*, mmNets'19, p. 51–56, New York, NY, USA, 2019. Association for Computing Machinery.

[Stu22] Frolic Studio. "Smartians.", 2022. Last accessed 12 May 2022.

[Swi22] Switchbot. "SwitchBot Curtain.", 2022. Last accessed 24 April 2022.

[SZH12] Valkyrie Savage, Xiaohan Zhang, and Björn Hartmann. "Midas: fabricating custom capacitive touch sensors to prototype interactive objects." In *Proceedings of the 25th annual ACM symposium on User interface software and technology*, pp. 579–588, 2012.

[Tes22] Tesla. "Electric Cars, Solar & Clean Energy — Tesla.", 2022. Last accessed 14 May 2022.

[TKF20] Md Farhan Tasnim Oshim, Julian Killingback, Dave Follette, Huaishu Peng, and Tauhidur Rahman. "MechanoBeat: Monitoring Interactions with Everyday Objects using 3D Printed Harmonic Oscillators and Ultra-Wideband Radar." In *Proceedings of the 33rd Annual ACM Symposium on User Interface Software and Technology*, pp. 430–444, 2020.

[TZW19] Sheng Tan, Linghan Zhang, Zi Wang, and Jie Yang. "MultiTrack: Multi-user tracking and activity recognition using commodity WiFi." In *Proceedings of the 2019 CHI Conference on Human Factors in Computing Systems*, pp. 1–12, 2019.

[VH10] Nicolas Villar and Steve Hodges. "The Peppermill: A human-powered user interface device." In *Proceedings of the fourth international conference on Tangible, embedded, and embodied interaction*, pp. 29–32, 2010.

[VSC16] Aggeliki Vlachostergiou, Georgios Stratogiannis, George Caridakis, George Siolas, and Phivos Mylonas. "User adaptive and context-aware smart home using pervasive and semantic technologies." *Journal of Electrical and Computer Engineering*, **2016**, 2016.

[WJC18] Hao Wang, Abbas Jasim, and Xiaodan Chen. "Energy harvesting technologies in roadway and bridge for different applications–A comprehensive review." *Applied energy*, **212**:1083–1094, 2018.

[WKO21] Ruiyu Wang, Paulo Valente Klaine, Oluwakayode Onireti, Yao Sun, Muhammad Ali Imran, and Lei Zhang. "Deep learning enabled beam tracking for non-line of sight millimeter wave communications." *IEEE Open Journal of the Communications Society*, **2**:1710–1720, 2021.

[WLC18] Weitian Wang, Rui Li, Yi Chen, Z. Max Diekel, and Yunyi Jia. "Facilitating Human-Robot Collaborative Tasks by Teaching-Learning-Collaboration From Human Demonstrations.", 2018.

[WLC21] Yuheng Wang, Haipeng Liu, Kening Cui, Anfu Zhou, Wensheng Li, and Huadong Ma. "m-activity: Accurate and real-time human activity recognition via millimeter wave radar." In *ICASSP 2021-2021 IEEE International Conference on Acoustics, Speech and Signal Processing (ICASSP)*, pp. 8298–8302. IEEE, 2021.

[WPM15] Muchen Wu, Parth H. Pathak, and Prasant Mohapatra. "Monitoring Building Door Events Using Barometer Sensor in Smartphones." In *Proceedings of the 2015 ACM International Joint Conference on Pervasive and Ubiquitous Computing*, UbiComp '15, p. 319–323, New York, NY, USA, 2015. Association for Computing Machinery.

[WTZ17] Zhiyi Wu, Jianhong Tang, Xin Zhang, and Zhicheng Yu. "An energy harvesting bracelet." *Applied Physics Letters*, **111**(1):013903, 2017.

[WWN16] Yuxi Wang, Kaishun Wu, and Lionel M Ni. "Wifall: Device-free fall detection by wireless networks." *IEEE Transactions on Mobile Computing*, **16**(2):581–594, 2016.

[WXZ20] Anandghan Waghmare, Qiuyue Xue, Dingtian Zhang, Yuhui Zhao, Shivan Mittal, Nivedita Arora, Ceara Byrne, Thad Starner, and Gregory D Abowd. "UbiquiTouch: Self sustaining ubiquitous touch interfaces." *Proceedings of the ACM on Interactive, Mobile, Wearable and Ubiquitous Technologies*, **4**(1):1–22, 2020.

[WZW16] Hao Wang, Daqing Zhang, Yasha Wang, Junyi Ma, Yuxiang Wang, and Shengjie Li. "RT-Fall: A real-time and contactless fall detection system with commodity WiFi devices." *IEEE Transactions on Mobile Computing*, **16**(2):511–526, 2016.

[WZW20] Chenshu Wu, Feng Zhang, Beibei Wang, and KJ Ray Liu. "msense: Towards mobile material sensing with a single millimeter-wave radio." *Proceedings of the ACM on Interactive, Mobile, Wearable and Ubiquitous Technologies*, **4**(3):1–20, 2020.

[WZW21] Fengyu Wang, Xiaolu Zeng, Chenshu Wu, Beibei Wang, and KJ Ray Liu. "mmHRV: Contactless heart rate variability monitoring using millimeter-wave radio." *IEEE Internet of Things Journal*, **8**(22):16623–16636, 2021.

[XCY17] Xi Xiong, Justin Chan, Ethan Yu, Nisha Kumari, Ardalan Amiri Sani, Changxi Zheng, and Xia Zhou. "Customizing Indoor Wireless Coverage via 3D-Fabricated Reflectors." In *Proceedings of the 4th ACM International Conference on Systems for Energy-Efficient Built Environments*, BuildSys '17, New York, NY, USA, 2017. Association for Computing Machinery.

[XJG22] Yucheng Xie, Ruizhe Jiang, Xiaonan Guo, Yan Wang, Jerry Cheng, and Yingying Chen. "mmEat: Millimeter wave-enabled environment-invariant eating behavior monitoring." *Smart Health*, **23**:100236, 2022.

[XLH14] Robert Xiao, Gierad Laput, and Chris Harrison. "Expanding the input expressivity of smartwatches with mechanical pan, twist, tilt and click." In *Proceedings of the SIGCHI Conference on Human Factors in Computing Systems*, pp. 193–196, 2014.

[YFS16] Hui-Shyong Yeo, Gergely Flamich, Patrick Schrempf, David Harris-Birtill, and Aaron Quigley. "Radarcat: Radar categorization for input & interaction." In *Proceedings of the 29th Annual Symposium on User Interface Software and Technology*, pp. 833–841, 2016.

[YGJ21] Zuozong Yin, Shiqiao Gao, Lei Jin, Shengkai Guo, Qinghe Wu, and Zezhang Li. "A shoe-mounted frequency up-converted piezoelectric energy harvester." *Sensors and Actuators A: Physical*, **318**:112530, 2021.

[YPZ16] Zhicheng Yang, Parth H Pathak, Yunze Zeng, Xixi Liran, and Prasant Mohapatra. "Monitoring vital signs using millimeter wave." In *Proceedings of the 17th ACM international symposium on mobile ad hoc networking and computing*, pp. 211–220, 2016.

[YPZ17] Zhicheng Yang, Parth H Pathak, Yunze Zeng, Xixi Liran, and Prasant Mohapatra. "Vital sign and sleep monitoring using millimeter wave." *ACM Transactions on Sensor Networks (TOSN)*, **13**(2):1–32, 2017.

[YSX22] Xiaoying Yang, Jacob Sayono, Jess Xu, Jiahao Nick Li, Josiah Hester, and Yang Zhang. "MiniKers: Interaction-Powered Smart Environment Automation." *Proc. ACM Interact. Mob. Wearable Ubiquitous Technol.*, **6**(3), sep 2022.

[YT10] Xiaodong Yang and Yingli Tian. "Robust door detection in unfamiliar environments by combining edge and corner features." In *2010 IEEE Computer Society Conference on Computer Vision and Pattern Recognition-Workshops*, pp. 57–64. IEEE, 2010.

[YZ21] Xiaoying Yang and Yang Zhang. "CubeSense: Wireless, Battery-Free Interactivity through Low-Cost Corner Reflector Mechanisms." In *Extended Abstracts of the 2021 CHI Conference on Human Factors in Computing Systems*, CHI EA '21, New York, NY, USA, 2021. Association for Computing Machinery.

[ZIJ19a] Yang Zhang, Yasha Iravantchi, Haojian Jin, Swarun Kumar, and Chris Harrison. "Sozu: Self-powered radio tags for building-scale activity sensing." In *Proceedings of the 32nd Annual ACM Symposium on User Interface Software and Technology*, pp. 973–985, 2019.

[ZIJ19b] Yang Zhang, Yasha Iravantchi, Haojian Jin, Swarun Kumar, and Chris Harrison. "Sozu: Self-Powered Radio Tags for Building-Scale Activity Sensing." In *Proceedings of the 32nd Annual ACM Symposium on User Interface Software and Technology*, UIST '19, p. 973–985, New York, NY, USA, 2019. Association for Computing Machinery.

[ZLA18] Mingmin Zhao, Tianhong Li, Mohammad Abu Alsheikh, Yonglong Tian, Hang Zhao, Antonio Torralba, and Dina Katabi. "Through-wall human pose estimation using radio signals." In *Proceedings of the IEEE Conference on Computer Vision and Pattern Recognition*, pp. 7356–7365, 2018.

[ZLH18] Yang Zhang, Gierad Laput, and Chris Harrison. "Vibrosight: Long-Range Vibrometry for Smart Environment Sensing." UIST '18, p. 225–236, New York, NY, USA, 2018. Association for Computing Machinery.

[ZPZ20a] Dingtian Zhang, Jung Wook Park, Yang Zhang, Yuhui Zhao, Yiyang Wang, Yunzhi Li, Tanvi Bhagwat, Wen-Fang Chou, Xiaojia Jia, Bernard Kippelen, et al. "OptoSense: Towards ubiquitous self-powered ambient light sensing surfaces." *Proceedings of the ACM on Interactive, Mobile, Wearable and Ubiquitous Technologies*, **4**(3):1–27, 2020.

[ZPZ20b] Dingtian Zhang, Jung Wook Park, Yang Zhang, Yuhui Zhao, Yiyang Wang, Yunzhi Li, Tanvi Bhagwat, Wen-Fang Chou, Xiaojia Jia, Bernard Kippelen, et al. "OptoSense: Towards ubiquitous self-powered ambient light sensing surfaces." *Proceedings of the ACM on Interactive, Mobile, Wearable and Ubiquitous Technologies*, **4**(3):1–27, 2020.

[ZWX19] Youwei Zeng, Dan Wu, Jie Xiong, Enze Yi, Ruiyang Gao, and Daqing Zhang. "FarSense: Pushing the range limit of WiFi-based respiration sensing with CSI ratio of two antennas." *Proceedings of the ACM on Interactive, Mobile, Wearable and Ubiquitous Technologies*, **3**(3):1–26, 2019.

[ZYH18] Yang Zhang, Chouchang (Jack) Yang, Scott E. Hudson, Chris Harrison, and Alanson Sample. "Wall++: Room-Scale Interactive and Context-Aware Sensing." In

Proceedings of the 2018 CHI Conference on Human Factors in Computing Systems, CHI '18, p. 1–15, New York, NY, USA, 2018. Association for Computing Machinery.

[ZYS14] Chen Zhao, Sam Yisrael, Joshua R Smith, and Shwetak N Patel. "Powering wireless sensor nodes with ambient temperature changes." In *Proceedings of the 2014 ACM international joint conference on pervasive and ubiquitous computing*, pp. 383–387, 2014.

[ZZK18] AI Zakharov, LN Zakharova, and MG Krasnogorskii. "Monitoring landslide activity by radar interferometry using trihedral corner reflectors." *Izvestiya, Atmospheric and Oceanic Physics*, **54**:1110–1120, 2018.

[ZZX22] Jia Zhang, Yinian Zhou, Rui Xi, Shuai Li, Junchen Guo, and Yuan He. "AmbiEar: MmWave Based Voice Recognition in NLoS Scenarios." *Proc. ACM Interact. Mob. Wearable Ubiquitous Technol.*, **6**(3), sep 2022.